

A Multiresolution approach to solve large-scale optimization problems

Rosa Donat*, Sergio López-Ureña*

July 26, 2022

Abstract

General purpose optimization techniques can be used to solve many problems in engineering computations, although their cost is often prohibitive when the number of degrees of freedom is very large. We describe a multilevel approach to speed up the computation of the solution of a large-scale optimization problem by a given optimization technique. By embedding the problem within Harten’s Multiresolution Framework (MRF), we set up a procedure that leads to the desired solution, after the computation of a finite sequence of *sub-optimal solutions*, which solve auxiliary optimization problems involving a smaller number of variables. For convex optimization problems having *smooth* solutions, we prove that the distance between the optimal solution and each sub-optimal approximation is related to the accuracy of the interpolation technique used within the MRF and analyze its relation with the performance of the proposed algorithm. Several numerical experiments confirm that our technique provides a computationally efficient strategy that allows the end user to treat both the optimizer and the objective function as black boxes throughout the optimization process.

1 Introduction

Optimization problems of the type

$$\text{Find } z_{\min} \in \mathbb{R}^N \text{ such that } F(z_{\min}) = \min_{z \in \mathbb{R}^N} F(z), \quad N \gg 1, \quad (1)$$

arise frequently in applications, often in connection with the context of calculus of variations, PDE constrained optimization, optimal control [8, 9, 25] or image processing [11, 10].

In many occasions, specially in engineering computations, it is known, a priori, that the problem has a unique solution which can be computed (from a given initial data) with an appropriate ‘off-the-shelf’ (black-box type) optimization technique which, however, tends to be very time consuming. Assuming that problem eq. (1) can be solved by using a given optimization technique, \mathcal{D} , we describe a strategy to reduce the computational time required by the direct application of \mathcal{D} on a space with N degrees of freedom. Our technique is based on embedding problem eq. (1) in Harten’s Multiresolution Framework (MRF henceforth) [27], which can be loosely described as a set of mathematical tools to obtain multilevel representations of discrete data sets, similar to those obtained in the well known wavelet framework.

*Universitat de València, 50th Doctor Moliner street, Burjassot (Spain) (donat@uv.es, sergio.lopez-urena@uv.es). The authors have been supported by grant MTM2017-83942 funded by Spanish MINEC and by grant PID2020-117211GB-I00 funded by MCIN/AEI/10.13039/501100011033.

Harten’s MRF has been successfully applied for different purposes and in several scenarios (see e.g. [18, 1, 5, 14, 13, 7]) but, to the best of our knowledge, the applications carried out in [19, 28] constitute the first attempt to use Harten’s MRF in connection with constrained/unconstrained optimization. The aim of this paper is to provide a complete mathematical description of the technique used in [19, 28] to solve large-scale optimization problems of the type eq. (1), together with some theoretical results on its properties and performance, including several numerical experiments that confirm our theoretical analysis. Our technique will be referred throughout the paper as MR/OPT (for *Multiresolution for Optimization*).

1.1 Related Work

The use of multilevel techniques to solve large-scale optimization problems has been a common trend in the literature since the mid 80’s. Largely fueled by the success of multigrid methods as efficient solvers for discretized partial differential equations (PDE) [8, 9, 25]) and the fact that many large-scale optimization problems arise from the discretization of a PDE [30, 15, 12, 22, 23, 24], there are nowadays many multilevel algorithms which exploit the fact that, if eq. (1) comes from an underlying infinite dimensional problem, it may be described at several discretization levels.

The idea behind many of these multilevel optimization techniques is to combine an iterative (or descent) method with a correction which requires the solution of a reduced, lower dimensional, auxiliary problem which is cheaper to solve. For example, in the MG/OPT framework introduced by Nash in [30], the solutions of low-dimensional problems (*coarse resolution* problems) are used to compute search directions for higher dimensional problems in a multigrid fashion, an idea that has been considered by Frandi and Papini in a series of papers [22, 23] where derivative-free multilevel optimization techniques are considered. Other techniques, such as the *trust-region* multilevel optimization also make use of auxiliary, lower dimensional, optimization problems (or *surrogate models* [22, 23]) which make an explicit use of the family of discrete versions, at different resolution levels, associated to the infinite-dimensional/continuous problem.

The present paper describes a different strategy to solve eq. (1), which is close, in spirit, to the so-called ‘*cost-effective*’ multiscale strategy used in [13], whose objective is to reduce the cost of using a time-consuming numerical scheme on a fine-mesh simulation involving hyperbolic PDEs. Our aim is not to design a new optimization algorithm, but rather to speed up the computation carried out by a convenient (but possibly very time-consuming) optimization technique, starting at a given initial guess provided by the end-user.

In the MR/OPT algorithm, the function F in eq. (1) and the optimization tool are treated as black boxes, with the only requirement that \mathcal{D} is appropriate to solve eq. (1) (except for the possibly very large computational expense). Its design involves the computation of a sequence of iterates, which solve *auxiliary optimization problems* in \mathbb{R}^m ($m < N$) which do not make use of any discretization of the underlying infinite-dimensional problem at lower resolution levels (in contrast with [15, 22, 23, 24]). Somewhat related multilevel optimization strategies can be found in e.g. [19, 26, 29] (and references therein) in the context of aerodynamic shape optimization, where it is now recognized that a shape optimization problem can be solved as a sequence of optimization steps that evolve from a basic parametrization of the shape to more refined parametrizations. These techniques are capable of implementing geometry changes while maintaining the required constraints and obtaining an improvement in the efficiency, accuracy, and robustness of widely used optimization procedures. As in the MR/OPT strategy, they are not based on discretizing the underlying infinite dimensional problem at several accuracy levels.

The paper is organized as follows: In section 2 we briefly recall the main ingredients of Harten’s MRF required for the description of the MR/OPT strategy, which is carefully described in section 3.

In section 2.1, we describe the interpolatory MR setting, including the specific prediction schemes used in the numerical examples of section 4, chosen to illustrate the performance and limitations of our technique. We finish with some conclusions and perspectives in section 5.

2 Harten's Framework For Multiresolution

In this section we shall recall the essential ingredients of Harten's MRF which are required for the description of our algorithm (for a complete description of Harten's MRF see e.g. [27, 2, 3]).

A distinctive characteristic of Harten's approach is that the discrete data at different resolution levels in a specific MRF are assumed to come from a particular *discretization* procedure, acting on an appropriate functional space, which is 'naturally' linked to a hierarchy of *nested meshes*¹ $(\mathcal{G}^k)_{k=0}^L$ covering a fixed spatial domain.

Assuming that N_k is the dimension of the discrete data attached to \mathcal{G}^k , where $N_L > N_{L-1} > \dots > N_0$, a multiresolution (MR) representation of a discrete data set, $z^L \in \mathbb{R}^{N_L}$, is an *equivalent representation* (in \mathbb{R}^{N_L}) which consists in a *coarse* representation of this data set, $z^0 \in \mathbb{R}^{N_0}$, together with a sequence of *details*, $d^\ell \in \mathbb{R}^{N_{\ell+1}-N_\ell}$, $\ell = 0, \dots, L-1$, that can be understood as 'essential' (non-redundant) difference in information between consecutive resolution levels.

In a nutshell, Harten's MRF can be described as follows: For each pair of consecutive resolution levels, we are given a *decimation operator* D_k^{k-1} , which extracts $k-1$ level information from the discrete data at level k , and a *prediction operator* P_{k-1}^k which produces k level data from $k-1$ level information. D_k^{k-1} is a linear operator, fully determined by the underlying discretization procedure that defines the framework. P_{k-1}^k may be linear or nonlinear². These two operators are required to satisfy a *consistency relation* at all resolution levels (I_ℓ is the identity operator on \mathbb{R}^{N_ℓ}):

$$D_k^{k-1} P_{k-1}^k = I_{k-1}, \quad (2)$$

(but $P_{k-1}^k D_k^{k-1} \neq I_k$). Notice that, for $z^k \in \mathbb{R}^{N_k}$ we can write

$$z^k = P_{k-1}^k D_k^{k-1} z^k + (I_k - P_{k-1}^k D_k^{k-1}) z^k = P_{k-1}^k z^{k-1} + e^k,$$

hence each $z^k \in \mathbb{R}^{N_k}$ can be *represented* in terms of a 'decimated' version (at the next, coarser, resolution level) together with a 'prediction error', i.e.

$$z^k \equiv \begin{cases} z^{k-1} & := D_k^{k-1} z^k \in \mathbb{R}^{N_{k-1}}, \\ e^k & := z^k - P_{k-1}^k z^{k-1} \in \mathbb{R}^{N_k}. \end{cases} \quad (3)$$

The consistency relation eq. (2) implies that $D_k^{k-1} e^k = 0$, so that the representation of z^k in terms of (z^{k-1}, e^k) specified in eq. (3) (with $N_{k-1} + N_k$ components) is redundant. The *details* d^{k-1} represent exactly the non-redundant information contained in e^k , so that a one-to-one correspondence between z^k and (z^{k-1}, d^{k-1}) can be established (hence $d^{k-1} \in \mathbb{R}^{N_k - N_{k-1}}$). By iterating this procedure from level L to level 1, we obtain the full MR representation of $z^L \in \mathbb{R}^{N_L}$:

$$z^L \leftrightarrow (z^{L-1}, d^{L-1}) \leftrightarrow (z^{L-2}, d^{L-2}, d^{L-1}) \leftrightarrow \dots \leftrightarrow (z^0, d^0, \dots, d^{L-1}). \quad (4)$$

In eq. (4), $z^k = D_{k+1}^k \dots D_L^{L-1} z^L \in \mathbb{R}^{N_k}$, $L > k \geq 0$, i.e. z^k are coarse versions of z^L at the different resolution levels, obtained by successive decimation. Moreover, the details d^{k-1} are related to the

¹ $\{\mathcal{G}^k\}_k$ is nested if $\mathcal{G}^k \subset \mathcal{G}^{k+1}$

²This is a major difference between Harten's MRF and the classical wavelet theory.

prediction error $e^k = (I - P_{k-1}^k D_k^{k-1})z^k$, and provide information on the local smoothness of the function which is associated to the discrete data z^L by the discretization operator which defines the framework (see also section 2.1).

If we denote by $M_{m,j}$ ($m < j$) the multiresolution transform operator that acts between the resolution levels m and j , then, for $0 \leq \ell \leq k \leq L$ and $\forall z^L \in \mathbb{R}^{N_L}$,

$$M_k^L z^L = (z^k, d^k, \dots, d^{L-1}) \quad \rightarrow \quad M_\ell^L z^L = (M_\ell^k z^k, d^k, \dots, d^{L-1}), \quad (5)$$

or, equivalently,

$$M_{\ell,L} z^L = (z^\ell, d^\ell, \dots, d^{k-1}, d^k, \dots, d^{L-1}) \equiv \begin{cases} M_{k,L} z^L = (z^k, d^k, \dots, d^{L-1}), \\ M_{\ell,k} z^k = (z^\ell, d^\ell, \dots, d^{k-1}). \end{cases} \quad (6)$$

We shall use these relations in various places throughout the paper.

An important property for the practical use of MR transformations is their *stability* with respect to *perturbations*. In this paper, we shall assume that the prediction operators $P_{k-1}^k : \mathbb{R}^{N_{k-1}} \rightarrow \mathbb{R}^{N_k}$ are linear (they can be represented as $\mathbb{R}^{N_k \times N_{k-1}}$ matrices) which implies in turn that the multiscale transformations $M_{m,j} : \mathbb{R}^{N_j} \rightarrow \mathbb{R}^{N_m}$ are also a linear operators ($\mathbb{R}^{N_j \times N_m}$ matrices). In this case, the stability of the associated MRF can be stated as follows

$$\|M_{m,j}\|_\infty \leq C, \quad \|M_{m,j}^{-1}\|_\infty \leq \tilde{C}, \quad (7)$$

with C, \tilde{C} independent of m, j or L , for $0 \leq m \leq j \leq L$, and $\|\cdot\|_\infty$ the usual operator norm.

Within Harten's framework, stability is related to the *convergence* of the process that results from the recursive application of the prediction operators, which involves a refinement process akin to those found in the theory of subdivision refinement³. The prediction operators considered in this paper satisfy a property which guarantees the stability of the associated MR transformations. This property, which we shall denote as *Property S*, is defined below.

Definition 1 (Property S). Let $\mathcal{P} = \{P_k^{k+1}\}_{k=0}^\infty$ be a sequence of linear prediction operators. We will say that \mathcal{P} satisfies *property S* if there exist $d_1, d_2 > 0$, such that for any $0 \leq \ell < k$

$$d_1 \|z^\ell\|_\infty \leq \|P_\ell^k z^\ell\|_\infty \leq d_2 \|z^\ell\|_\infty, \quad \forall z^\ell \in \mathbb{R}^{N_\ell}, \quad (8)$$

where $P_\ell^k := P_{k-1}^k \dots P_{\ell+1}^{\ell+2} P_\ell^{\ell+1}$ is the operator that computes the recursive prediction process between levels $l < k$.

Remark.. We shall assume that $P_k^k = I_k$. Notice that

$$z^L = P_k^L z^k \quad \Leftrightarrow \quad M_{k,L} z^L = (z^k, 0, \dots, 0). \quad (9)$$

2.1 Harten's Interpolatory MRF

In this paper, we shall use Harten's interpolatory MR framework, which is characterized by the assumption that the discrete data correspond to the point-evaluations of a function, defined on the spatial domain underlying the nested mesh structure.

We briefly describe next the one-dimensional case: Let us consider the sequence of nested meshes on the interval $[0, 1]$ obtained by the dyadic refinement of a uniform mesh \mathcal{G}^0 , with grid spacing

³The convergence theory of these processes is outside the scope of this paper. The reader is referred to [20] for the concept of convergence in subdivision refinement.

$h_0 = 1/J_0$. Thus, $\mathcal{G}^k = \{ih_k\}_{i=0}^{J_k}$ with $h_k = h_0/2^k = 1/J_k$ and the k -th level information consists in $N_k = J_k + 1$ discrete values, for each k , $0 \leq k \leq L$.

The operators that define the transfer of information between two consecutive resolution levels (k fine, $k-1$ coarse) in the 1D interpolatory MRF are as follows:

- *Decimation by downsampling*: For $z^k \in \mathbb{R}^{N_k}$,

$$z_i^{k-1} = (D_k^{k-1} z^k)_i = z_{2i}^k, \quad 0 \leq i \leq J_{k-1}. \quad (10)$$

Notice that this decimation operator corresponds to the interpretation of the discrete data as the point-values of an underlying function defined on the unit interval $[0, 1]$ at each resolution level. Obviously $z^{k-1} \in \mathbb{R}^{N_{k-1}}$ is a *coarse* version of the data z^k , which corresponds to the point-values of the function on the grid \mathcal{G}^{k-1} .

- *Prediction by interpolation*. Because of eq. (10), the consistency relation eq. (2) becomes

$$z_i^{k-1} = (D_k^{k-1} P_{k-1}^k z^{k-1})_i = (P_{k-1}^k z^{k-1})_{2i}.$$

This *interpolation condition* implies that the prediction errors at even points are zero, thus, only the predicted values at odd grid points need to be computed and stored. Then, the one-to-one correspondence between the discrete sets z^k and (z^{k-1}, d^{k-1}) , i.e. the two-level multiresolution transformation $M_{k-1,k}$ and its inverse, are

$$M_{k-1,k} z^k = (z^{k-1}, d^{k-1}) \leftrightarrow \begin{cases} z_i^{k-1} = z_{2i}^k, & 0 \leq i \leq J_{k-1}, \\ d_i^{k-1} = z_{2i-1}^k - (P_{k-1}^k z^{k-1})_{2i-1}, & 1 \leq i \leq J_{k-1}, \end{cases} \quad (11)$$

$$M_{k-1,k}^{-1} (z^{k-1}, d^k) = z^k \leftrightarrow \begin{cases} z_{2i}^k = z_i^{k-1}, & 0 \leq i \leq J_{k-1}, \\ z_{2i-1}^k = d_i^{k-1} + (P_{k-1}^k z^{k-1})_{2i-1}, & 1 \leq i \leq J_{k-1}. \end{cases} \quad (12)$$

Remark. From eq. (11), since $z^{k-1} = D_k^{k-1} z^k$, $z^k = D_{k+1}^k \cdots D_L^{L-1} z^L$, we can also write $d_i^{k-1} = d_i^{k-1}(z^L)$, which clearly express that the detail coefficients are determined by the properties of the discrete data at the finest resolution level.

In this paper, we shall consider prediction operators based on certain piecewise polynomial interpolatory techniques of fixed polynomial degree, n , odd. We refer the reader to [3, 16] for specific details, and simply provide the prediction rules for $n = 1, 3, 5$

$$\begin{cases} (P_{k-1}^k z^{k-1})_{2i-1} = \sum_{\ell=1}^{(n+1)/2} \beta_\ell (z_{i+\ell}^{k-1} + z_{i+1-\ell}^{k-1}), & \frac{n+1}{2} \leq i \leq J_{k-1} - \frac{n-1}{2}, \\ (P_{k-1}^k z^{k-1})_{2i} = z_i^{k-1}, & 0 \leq i \leq J_{k-1}, \end{cases} \quad (13)$$

$$\begin{cases} n = 1 \Rightarrow \beta_1 = 1/2, \\ n = 3 \Rightarrow \beta_1 = 9/16, \beta_2 = -1/16, \\ n = 5 \Rightarrow \beta_1 = 150/256, \beta_2 = -25/256, \beta_3 = 3/256, \end{cases} \quad (14)$$

with the following *special boundary rules* at the left boundary of $[0, 1]$ for $n = 3$,

$$(P_{k-1}^k z^{k-1})_1 = \frac{5}{16} z_0^{k-1} + \frac{15}{16} z_1^{k-1} - \frac{5}{16} z_2^{k-1} + \frac{1}{16} z_3^{k-1}, \quad (15)$$

and $n = 5$,

$$\begin{cases} (P_{k-1}^k z^{k-1})_1 = \frac{63}{256} z_0^{k-1} + \frac{315}{256} z_1^{k-1} - \frac{105}{128} z_2^{k-1} + \frac{63}{128} z_3^{k-1} - \frac{45}{256} z_4^{k-1} + \frac{7}{256} z_5^{k-1}, \\ (P_{k-1}^k z^{k-1})_3 = -\frac{7}{256} z_0^{k-1} + \frac{105}{256} z_1^{k-1} + \frac{105}{128} z_2^{k-1} - \frac{35}{128} z_3^{k-1} + \frac{21}{256} z_4^{k-1} - \frac{3}{256} z_5^{k-1}. \end{cases} \quad (16)$$

The corresponding rules at the right end of $[0, 1]$ can be obtained by symmetry. We prove in the Appendix that these prediction operators satisfy *property S* with $d_1 = 1$, hence, the associated MR transformations are stable, i.e. satisfy eq. (7).

Remark. The prediction operators defined by eq. (13) are related to the well known (stationary⁴) subdivision rules of the interpolatory Deslauriers-Dubuc subdivision schemes [20, 16] for infinite sequences. To deal with bounded domains, we have to take care of the, possibly special, prediction rules close to the boundaries, where the required centered stencils might leave the domain. For $n = 1$, i.e. linear interpolation, only the boundary values $z_0^{k-1}, z_{N_{k-1}}^{k-1}$ are required to apply the prediction operator specified in eq. (13) at each resolution level, hence no special rules are required close to the boundaries of the domain. However, for $n = 3$ (or $n = 5$) interpolation polynomials of degree 3 (or 5) are involved, hence special rules are required to predict k -data from data from $(k - 1)$ -th grid values at the positions $i = 1$ and $i = J_{k-1} - 1$ (or $i = 1, 2, i = J_{k-1} - 1, J_{k-1} - 2$ for $n = 5$). To obtain eqs. (15) and (16), we have used the stencil of the $n + 1$ points closest to the boundary, in order to obtain the required predicted value [3]. Hence, all polynomial pieces in the interpolatory reconstruction process have the same degree (and the same approximation order).

The decay of the scale coefficients with respect to the resolution level under smoothness assumptions, is a well known fact that is very simple to explain in the interpolatory MRF. Since the details are interpolation errors, their size (and behavior across scales) is determined by the approximation order of the interpolatory technique used to define the prediction operators. The rules in eqs. (13) to (16), involve polynomials of degree n , hence

$$d_i^{k-1} = \mathcal{O}(h_k^{n+1}). \quad (17)$$

when the data around the spatial location corresponding to the indices $(2i - 1, k)$ correspond to the point values of a sufficiently smooth function.

In this paper, we shall make use of the 1D interpolatory MRF just described and its 2D version obtained by using a tensor-product approach [6]. When using the 1D prediction operators specified above in the 2D tensor-product context, the prediction operators have the same order of approximation, with respect to the uniform mesh spacing of the (tensor product) hierarchical mesh structure, as in the 1D setting. Hence, the decay of the scale coefficients in the 2D tensor-product interpolatory MRF is also given by eq. (17).

3 MR/OPT: A multiresolution approach for the efficient solution of large-scale optimization problems

We shall describe next a multilevel strategy to compute the solution of eq. (1), assuming that the end-user provides an initial guess \bar{z} and a preferred optimization tool \mathcal{D} so that

$$z_{\min} = \mathcal{D}(\bar{z}, F, N) = \arg \min\{F(z), z \in \mathbb{R}^N\}. \quad (18)$$

The notation above is meant to emphasize the fact that the optimization problem eq. (1), with F as the objective function on a discrete space with N degrees of freedom, can be solved using \mathcal{D} as optimization tool and \bar{z} as the initial guess.

Considering $N = N_L$ as the finest resolution level in a sequence of $L + 1$ levels of refinement corresponding to discrete spaces \mathbb{R}^{N_k} ($N_0 < N_1 < \dots < N_L = N, L > 0$) within a MRF which

⁴Stationary subdivision rules are independent of the refinement level.

is *appropriate* for the given problem, the MR/OPT strategy produces a sequence of ‘*sub-optimal*’ solutions, $\{z^{L,k}\}_{k=0}^{L+1}$, satisfying

$$z^{L,0} := \bar{z}, \quad F(\bar{z}) = F(z^{L,0}) \geq F(z^{L,1}) \geq \dots \geq F(z^{L,L+1}), \quad z^{L,L+1} = z_{\min}. \quad (19)$$

The k -th level sub-optimal solution satisfies

$$F(z^{L,k+1}) = \min\{F(z), z \in \Xi_k\}$$

where Ξ_k is a subset of \mathbb{R}^N , whose construction depends on the MRF being used and on the sequence of prediction operators \mathcal{P} .

In this paper we always assume that the prediction operators in \mathcal{P} are linear and satisfy *property S*. Hence the MR transformations used are also linear operators and eq. (7) is satisfied.

At the coarsest resolution level ($k = 0$) we set $z^{L,0} := \bar{z}$, the initial guess provided by the user. Its MR representation, $M_{0,L}z^{L,0} = M_{0,L}\bar{z} =: (\bar{z}^0, \bar{d}^0, \dots, \bar{d}^{L-1})$, serves to define the set $\Xi_0 \subset \mathbb{R}^{N_L}$ and the associated 0-th-level *objective function* as follows

$$\begin{aligned} \Xi_0 &:= \{M_{0,L}^{-1}(\bar{z}^0 + \varepsilon^0, \bar{d}^0, \dots, \bar{d}^{L-1}), \varepsilon^0 \in \mathbb{R}^{N_0}\}, \\ F_0(\varepsilon^0) &:= F(M_{0,L}^{-1}(\bar{z}^0 + \varepsilon^0, \bar{d}^0, \bar{d}^1, \dots, \bar{d}^{L-1})), \quad \varepsilon^0 \in \mathbb{R}^{N_0}. \end{aligned}$$

Since the MR operators are linear, taking into account eq. (9), we can write

$$M_{0,L}^{-1}(\bar{z}^0 + \varepsilon^0, \bar{d}^0, \bar{d}^1, \dots, \bar{d}^{L-1}) = \bar{z} + P_0^L \varepsilon^0.$$

Hence Ξ_0 is an affine space with N_0 degrees of freedom, which is defined by considering only perturbations (of the MR representation) of the initial data at the coarsest resolution level. These perturbations are moved to \mathbb{R}^{N_L} by successive prediction.

We then compute (assuming it is feasible⁵)

$$\varepsilon_*^0 := \arg \min\{F_0(\varepsilon^0), \varepsilon^0 \in \mathbb{R}^{N_0}\} = \mathcal{D}(0, F_0, N_0), \quad (20)$$

and define the *sub-optimal solution at level 0* as

$$z^{L,1} := \bar{z} + P_0^L \varepsilon_*^0 = z^{L,0} + P_0^L \varepsilon_*^0. \quad (21)$$

Obviously

$$z^{L,1} = \arg \min\{F(z), z \in \Xi_0\}, \quad F(z^{L,1}) = F_0(\varepsilon_*^0) \leq F_0(0) = F(z^{L,0}) = F(\bar{z}).$$

Notice that the computation of $z^{L,1}$ can be carried out involving only direct calls to the objective function F , since $F_0(\varepsilon^0) = F(\bar{z} + P_0^L \varepsilon^0)$. Notice that the user only needs to provide F , and the MRF takes care of the definition of the objective function F_0 . In addition, considering $\varepsilon^0 = 0 \in \mathbb{R}^{N_0}$ as the initial guess to solve eq. (20) (the *0-th level auxiliary optimization problem*) corresponds to considering $z^{L,0} = \bar{z}$ as the ‘corresponding’ initial guess in the affine space $\Xi_0 \subset \mathbb{R}^N$. Notice also that

$$M_{0,L}z^{L,1} = M_{0,L}\bar{z} + M_{0,L}P_0^L \varepsilon_*^0 = (\bar{z}^0 + \varepsilon_*^0, \bar{d}^0, \dots, \bar{d}^{L-1}),$$

i.e. the difference between $z^{L,0}$ and $z^{L,1}$ occurs only at the coarsest resolution level, while the ‘details’ in their MR representations coincide at all higher resolution levels. Taking into account eq. (5), we can write

$$M_{1,L}z^{L,1} = (z_*^1, \bar{d}^1, \dots, \bar{d}^L), \quad M_{0,1}z_*^1 = (\bar{z}_0 + \varepsilon_0^*, \bar{d}^0) \equiv z_*^1 = M_{0,1}^{-1}(\bar{z}_0, \bar{d}^0) + P_0^1 \varepsilon_0^0$$

⁵We shall see that this is indeed the case for convex optimization problems.

so that we can repeat the process as if the level 1 was the coarsest resolution level.

The general k -th step of the algorithm, $1 \leq k \leq L$, which will provide the *sub-optimal solution* $z^{L,k+1}$, can be described as follows: We assume that we have obtained $\varepsilon_*^m \in \mathbb{R}^{N_m}$, $0 \leq m \leq k-1$ (the solution of the m -th level auxiliary optimization problem) and the associated sub-optimal solutions, $\{z^{L,m}\}_{m=1}^k$, which satisfy the following properties ($\bar{z} = z^{L,0}$)

$$z^{L,m} = z^{L,m-1} + P_{m-1}^L \varepsilon_*^{m-1}; \quad M_{m,L} z^{L,m} = (z_*^m, \bar{d}^m, \dots, \bar{d}^{L-1}), \quad 1 \leq m \leq k,$$

where $z_*^0 = \bar{z}^0$ and

$$\begin{cases} z_*^m &= M_{m-1,m}^{-1}(z_*^{m-1}, \bar{d}^{m-1}) + P_{m-1}^m \varepsilon_*^{m-1}, \\ \bar{d}^j &= d^j(\bar{z}), \quad m-1 \leq j \leq L-1. \end{cases}$$

Then, we proceed as follows:

1. Consider the k -th level space of approximation

$$\Xi_k := \{M_{k,L}^{-1}(z_*^k + \varepsilon^k, \bar{d}^k, \dots, \bar{d}^{L-1}), \varepsilon^k \in \mathbb{R}^{N_k}\} = z^{L,k} + \{P_k^L \varepsilon^k, \varepsilon^k \in \mathbb{R}^{N_k}\} \quad (22)$$

which is an affine space in \mathbb{R}^N with N_k degrees of freedom.

2. Define the k -th level objective function $F_k : \mathbb{R}^{N_k} \rightarrow \mathbb{R}$,

$$F_k(\varepsilon^k) := F(M_{k,L}^{-1}(z_*^k + \varepsilon^k, \bar{d}^k, \dots, \bar{d}^{L-1})) = F(z^{L,k} + P_k^L \varepsilon^k). \quad (23)$$

Notice that only F and $\mathcal{P} = \{P_k^{k+1}\}_k$ is required to define F_k .

3. Assuming that it is feasible, compute the solution to the k -th level *auxiliary optimization problem*

$$\varepsilon_*^k := \arg \min\{F_k(\varepsilon^k), \varepsilon^k \in \mathbb{R}^{N_k}\} = \mathcal{D}(0, F_k, N_k). \quad (24)$$

4. Define

$$z^{L,k+1} := z^{L,k} + P_k^L \varepsilon_*^k. \quad (25)$$

Then, $z^{L,k+1} = \arg \min\{F(z), z \in \Xi_k\}$, $F(z^{L,k+1}) = F_k(\varepsilon_*^k) \leq F_k(0) = F(z^{L,k})$ and

$$M_{k,L} z^{L,k+1} = M_{k,L} z^{L,k} + M_{k,L} P_k^L \varepsilon_*^k = (z_*^{k+1} + \varepsilon_*^k, \bar{d}^k, \dots, \bar{d}^{L-1}) \quad (26)$$

hence

$$d^i(z^{L,k+1}) = \bar{d}^i = d^i(\bar{z}), \quad k \leq i \leq L-1, \quad (27)$$

$$M_{k+1,L} z^{L,k+1} = (z_*^{k+1}, \bar{d}^{k+1}, \dots, \bar{d}^{L-1}), \quad z_*^{k+1} := M_{k,k+1}^{-1}(z_*^k, \bar{d}^k) + P_k^{k+1} \varepsilon_*^k. \quad (28)$$

We can easily prove the following properties of the affine spaces Ξ_k .

Lemma 1. *The spaces Ξ_k in eq. (22) satisfy*

1. $\Xi_k \subset \Xi_{k+1}$, $0 \leq k < L$.
2. $\Xi_k = \{z^{L,\ell} + P_k^L \varepsilon^k : \varepsilon^k \in \mathbb{R}^{N_k}\}$, $\forall \ell, 0 \leq \ell \leq k \leq L$.

Proof. The Ξ_k are affine spaces, hence to prove item 1 it is enough to check that $P_k^L(\mathbb{R}^{N_k}) \subset P_{k+1}^L(\mathbb{R}^{N_{k+1}})$ and $z^{L,k} \in \Xi_{k+1}$. For this, we simply notice that $\forall \varepsilon_k \in \mathbb{R}^{N_k}$

$$P_k^L \varepsilon^k = P_{k+1}^L P_k^{k+1} \varepsilon^k, \quad z^{L,k} = z^{L,k+1} - P_{k+1}^L P_k^{k+1} \varepsilon_*^k, \quad P_k^{k+1} \varepsilon^k \in \mathbb{R}^{N_{k+1}}.$$

Since $z^{L,\ell} \in \Xi_\ell \subset \Xi_k$, item 2 follows immediately. \square

Remark. By construction, $\Xi_L = \mathbb{R}^{N_L} = \mathbb{R}^N$, hence $z^{L,L+1} = z_{\min}$ and the relations in eq. (19) are obviously satisfied.

The MR/OPT strategy substitutes the direct computation of the original (large-scale) optimization problem, by the computation of the solutions of a sequence of auxiliary optimization problems, each one of them associated to a level of refinement in a multiresolution ladder. It is reasonable to assume, when these auxiliary optimization problems admit a solution, it will be obtained *quite fast* at low resolution levels, due to the reduced number of degrees of freedom in the spaces where they are defined. In addition, it is expected that if the distance between the sub-optimal solutions and the true solution gets smaller while climbing up the MR ladder, then, even though each *auxiliary* minimization problem in the MR ladder involves an increasing number of variables, it is also expected that the improved initial guess (the previous sub-optimal solution) chosen to carry out the optimization process will improve the performance of the optimizer. In this case, the MR/OPT strategy leads to an overall gain in functional evaluations.

In the following section, we shall see that, in some cases, it is possible to ensure that the auxiliary optimization problems are of the same type as the original one, hence their solution can be computed by the same optimization technique, \mathcal{D} . In addition, we shall see that the previous observations on the performance of the MR/OPT strategy can be theoretically justified in some cases.

3.1 Some theoretical results on MR/OPT

We have assumed that the auxiliary optimization problems can be solved with the same optimization tool as the full problem eq. (18). It is simple to see that this is the case for quadratic minimization problems of the type

$$\text{Find } z_{\min} \in \mathbb{R}^N \text{ such that } F(z_{\min}) = \min_{z \in \mathbb{R}^N} F(z), \quad F(z) = \frac{1}{2} z^T A z - b^T z + c. \quad (29)$$

with A a symmetric and positive definite matrix.

Proposition 1. *Let us consider the quadratic minimization problem eq. (29), with A symmetric and positive definite. If the prediction operators in \mathcal{P} satisfy eq. (8), then the auxiliary minimization problem at level k eq. (24) is also a quadratic minimization problem of the same type.*

Proof. Using the definition of F in eq. (29), we have

$$\begin{aligned} F_k(\varepsilon^k) &= F(z^{L,k} + P_k^L \varepsilon^k) = \frac{1}{2} (z^{L,k} + P_k^L \varepsilon^k)^T A (z^{L,k} + P_k^L \varepsilon^k) - b^T (z^{L,k} + P_k^L \varepsilon^k) + c \\ &= F(z^{L,k}) + \frac{1}{2} (P_k^L \varepsilon^k)^T A P_k^L \varepsilon^k + (z^{L,k})^T A P_k^L \varepsilon^k - b^T P_k^L \varepsilon^k \\ &= \frac{1}{2} (\varepsilon^k)^T (P_k^L)^T A P_k^L \varepsilon^k - ((P_k^L)^T (b - A z^{L,k}))^T \varepsilon^k + F(z^{L,k}). \end{aligned}$$

Hence,

$$F_k(\varepsilon^k) = \frac{1}{2} (\varepsilon^k)^T A_k \varepsilon^k - b_k^T \varepsilon^k + c_k, \quad \begin{cases} A_k = (P_k^L)^T A P_k^L \in \mathbb{R}^{N_k \times N_k}, \\ b_k = (P_k^L)^T (b - A z^{L,k}) \in \mathbb{R}^{N_k}, \\ c_k = F(z^{L,k}) \in \mathbb{R}. \end{cases} \quad (30)$$

Obviously A_k is symmetric. If A is positive definite, then A_k is also positive definite, since P_k^L is injective, by eq. (8):

$$\varepsilon^k \neq 0 \quad \longleftrightarrow \quad P_k^L \varepsilon^k \neq 0 \quad \longleftrightarrow \quad 0 < (P_k^L \varepsilon^k)^T A (P_k^L \varepsilon^k) = (\varepsilon^k)^T A_k \varepsilon^k.$$

□

These quadratic optimization problems are special cases of a larger class of objective functions for which the same property holds: The auxiliary optimization problems are of the same type as the original one.

Proposition 2. *Let $F : \mathbb{R}^{N^L} \rightarrow \mathbb{R}$ be. If the prediction operators in \mathcal{P} satisfy property S, the auxiliary functions $F_k : \mathbb{R}^{N^k} \rightarrow \mathbb{R}$ defined in eq. (23) satisfy:*

1. *If F is convex and/or $F \in \mathcal{C}^2(\mathbb{R}^{N^L}, \mathbb{R})$, then F_k is also convex and/or $F_k \in \mathcal{C}^2(\mathbb{R}^{N^k}, \mathbb{R})$.*
2. *If the hessian matrix $\nabla^2 F(\xi^L)$ is a positive definite matrix $\forall \xi^L \in \mathbb{R}^{N^L}$, then $\nabla^2 F_k(\xi^k)$ is a positive definite matrix $\forall \xi^k \in \mathbb{R}^{N^k}$.*
3. *If F is coercive, i.e. $\lim_{\|z^L\|_\infty \rightarrow \infty} F(z^L) = +\infty$, then F_k is coercive.*

Proof. Since P_k^L is a linear operator, the proof of item 1 follows easily from the expression of F_k in eq. (23). To prove item 2, let $\xi^k \in \mathbb{R}^{N^k}$ be and notice that $\forall \varepsilon^k \neq 0$,

$$(\varepsilon^k)^T \nabla^2 F_k(\xi^k) \varepsilon^k = (P_k^L \varepsilon^k)^T \nabla^2 F(z^{L,k} + P_k^L \xi^k) (P_k^L \varepsilon^k) > 0,$$

since $\varepsilon^k \neq 0 \rightarrow P_k^L \varepsilon^k \neq 0$, by eq. (8).

To prove item 3, let $0 < \eta \in \mathbb{R}$. Since F is coercive, $\exists \delta = \delta(F, \eta)$ such that $F(z^L) > \eta$, $\forall z^L \in \mathbb{R}^{N^L} : \|z^L\|_\infty > \delta$. Define $\delta' := d_1^{-1}(\delta + \|z^{L,k}\|_\infty)$, with d_1 in eq. (8). Then $\forall \varepsilon^k : \|\varepsilon^k\|_\infty > \delta'$ we have

$$\|z^{L,k} + P_k^L \varepsilon^k\|_\infty \geq \|P_k^L \varepsilon^k\|_\infty - \|z^{L,k}\|_\infty \geq d_1 \|\varepsilon^k\|_\infty - \|z^{L,k}\|_\infty > d_1 \delta' - \|z^{L,k}\|_\infty = \delta,$$

hence,

$$F_k(\varepsilon^k) = F(z^{L,k} + P_k^L \varepsilon^k) > \eta, \quad \forall \varepsilon^k : \|\varepsilon^k\|_\infty > \delta'.$$

□

The following results aim to estimate the difference between sub-optimal solutions. For the sake of completeness and ease of reference, we include the following technical lemma.

Lemma 2. *Let $F \in \mathcal{C}^2(\mathbb{R}^N, \mathbb{R})$ be a convex function, such that its Hessian matrix is always positive definite. Let $A \subset \mathbb{R}^N$ be a compact convex set and let $x_A \in A$ be such that $\nabla F(x_A) = 0$. Let $B \subset A$ be a compact convex set and $x_B = \arg \min\{F(x), x \in B\}$. Then there exists $c = c(A, F, \|\cdot\|) \geq 1$ such that*

$$\|x_A - x_B\| \leq c \operatorname{dist}_{\|\cdot\|}(x_A, B),$$

where $\operatorname{dist}_{\|\cdot\|}(x_A, B) = \min\{\|x - x_A\|, x \in B\}$, for any norm in \mathbb{R}^N .

Proof. Since $\nabla F(x_A) = 0$, $B \subset A$ and A is convex, for any $x \in B$, $\exists \xi_x \in A$ such that

$$F(x) - F(x_A) = \frac{1}{2}(x - x_A)^T \nabla^2 F(\xi_x)(x - x_A). \quad (31)$$

The properties of F and A allow us to define ρ_{\min} , ρ_{\max} as follows

$$\rho_{\min} := \min_{\xi \in A} \min_{x \neq 0} \frac{x^T \nabla^2 F(\xi) x}{\|x\|^2} > 0, \quad \rho_{\max} := \max_{\xi \in A} \max_{x \neq 0} \frac{x^T \nabla^2 F(\xi) x}{\|x\|^2} > 0,$$

so that

$$\rho_{\min} \|x\|^2 \leq x^T \nabla^2 F(\xi) x \leq \rho_{\max} \|x\|^2, \quad \forall \xi \in A, \forall x \in \mathbb{R}^N.$$

Let w be an arbitrary but fixed point in B . Since $F(x_B) \leq F(w)$, applying eq. (31) with $x = w$ and $x = x_B$ and using the inequalities above, we get

$$\frac{\rho_{\min}}{2} \|x_B - x_A\|^2 \leq F(x_B) - F(x_A) \leq F(w) - F(x_A) \leq \frac{\rho_{\max}}{2} \|w - x_A\|^2.$$

Then,

$$\|x_A - x_B\| \leq c \|x_A - w\|, \quad c := \sqrt{\rho_{\max}/\rho_{\min}}. \quad (32)$$

The result follows from observing that the last inequality is true for every $w \in B$. \square

Proposition 3. *Let $F \in \mathcal{C}^2(\mathbb{R}^{N_L}, \mathbb{R})$ be a convex coercive function such that $\nabla^2 F(\xi^L)$ is a positive definite matrix $\forall \xi^L \in \mathbb{R}^{N_L}$. If $\mathcal{P} = \{P_k^{k+1}\}_{k=0}^{L-1}$ satisfies property S, then the sub-optimal solutions $\{z^{L,k}\}_{k=1}^{L+1}$ in eq. (25) are well defined and unique. In addition, for any compact and convex set D which contains in its interior the sequence $\{z^{L,k}\}_{k=0}^{L+1}$, there exists $C = C(F, D, \mathcal{P}) > 0$ such that for $\ell, k: 0 \leq \ell \leq k < L$,*

$$\|z^{L,k+1} - z^{L,\ell+1}\|_\infty \leq C \operatorname{dist}_\infty(z^{L,k+1}, \Xi_\ell \cap D). \quad (33)$$

Proof. By proposition 2, ε_*^k in eq. (24) is uniquely defined, and, thus, so is $z^{L,k+1}$, for each k , $0 \leq k \leq L$.

Now, let ℓ, k be a pair of (fixed) indices, $0 \leq \ell \leq k \leq L$. From eq. (25), we can write

$$\begin{aligned} z^{L,k+1} &= z^{L,k} + P_k^L \varepsilon_*^k, & \varepsilon_*^k &= \arg \min\{F_k(\varepsilon^k), \varepsilon^k \in \mathbb{R}^{N_k}\}. \\ z^{L,\ell+1} &= z^{L,\ell} + P_\ell^L \varepsilon_*^\ell, & \varepsilon_*^\ell &= \arg \min\{F_\ell(\varepsilon^\ell), \varepsilon^\ell \in \mathbb{R}^{N_\ell}\}. \end{aligned}$$

Thus, since $P_\ell^L = P_k^L P_\ell^k$,

$$z^{L,k+1} - z^{L,\ell+1} = z^{L,k} - z^{L,\ell} + P_k^L (\varepsilon_*^k - P_\ell^k \varepsilon_*^\ell).$$

Since $\Xi_\ell \subset \Xi_k$, $\exists! \varepsilon_\ell^k : z^{L,\ell} = z^{L,k} + P_\ell^L \varepsilon_\ell^k$ ⁶. Hence we can write

$$z^{L,k+1} - z^{L,\ell+1} = P_k^L (\varepsilon_A^k - \varepsilon_B^k), \quad \begin{cases} \varepsilon_A^k &= \varepsilon_*^k - \varepsilon_\ell^k, \\ \varepsilon_B^k &= P_\ell^k \varepsilon_*^\ell. \end{cases} \quad (34)$$

Thus, by eq. (8),

$$\|z^{L,k+1} - z^{L,\ell+1}\|_\infty \leq d_2 \|\varepsilon_A^k - \varepsilon_B^k\|_\infty.$$

To estimate the right-hand-side of the above relation, we seek to apply lemma 2. For this, we consider D to be a compact and convex set which contains in its interior the sequence of iterates $\{z^{L,k}\}_{k=0}^{L+1}$, and define the sets

$$A_{\ell,k} := \{\varepsilon^k \in \mathbb{R}^{N_k} : z^{L,\ell} + P_k^L \varepsilon^k \in D\}, \quad B_{\ell,k} := \{\varepsilon^k \in A_{\ell,k} : \varepsilon^k = P_\ell^k \varepsilon^\ell, \varepsilon^\ell \in \mathbb{R}^{N_\ell}\}.$$

Since D is compact and convex, and the prediction operators are linear, $A_{\ell,k}$ and $B_{\ell,k}$ are compact and convex sets in \mathbb{R}^{N_k} . Notice that lemma 1 and eq. (8) imply that there are one-to-one correspondences between $A_{\ell,k} \Leftrightarrow \Xi_k \cap D$ and $B_{\ell,k} \Leftrightarrow \Xi_\ell \cap D$. The sets $\Xi_k \cap D$ and $\Xi_\ell \cap D$ are compact and convex in \mathbb{R}^{N_L} .

Taking into account the relations above, we easily get

$$z^{L,\ell+1} = z^{L,\ell} + P_\ell^L P_\ell^k \varepsilon_*^\ell \rightarrow \varepsilon_B^k \in B_{\ell,k}, \quad z^{L,k+1} = z^{L,\ell} + P_k^L \varepsilon_A^k \rightarrow \varepsilon_A^k \in A_{\ell,k}. \quad (35)$$

⁶It is unique because of eq. (8).

Hence, considering the function

$$F_{\ell,k} : \mathbb{R}^{N_k} \rightarrow \mathbb{R}, \quad F_{\ell,k}(\varepsilon^k) := F(z^{L,\ell} + P_k^L \varepsilon^k)$$

we have

$$F_{\ell,k}(\varepsilon_A^k) = F(z^{L,k+1}) = \min_{z^L \in \Xi_k} F(z^L), \quad F_{\ell,k}(\varepsilon_B^k) = F(z^{L,\ell+1}) = \min_{z^L \in \Xi_\ell} F(z^L),$$

therefore

$$F_{\ell,k}(\varepsilon_A^k) = \min_{\varepsilon^k \in A_{\ell,k}} F_{\ell,k}(\varepsilon^k), \quad F_{\ell,k}(\varepsilon_B^k) = \min_{\varepsilon^k \in B_{\ell,k}} F_{\ell,k}(\varepsilon^k).$$

Since $F_{\ell,k}(\varepsilon^k) = F_k(\varepsilon_\ell^k + \varepsilon^k)$, we have that $\nabla F_{\ell,k}(\varepsilon_A^k) = \nabla F_k(\varepsilon_\ell^k) = 0$. Hence, applying lemma 2, there exists $c_{\ell,k} = c_{\ell,k}(A_{\ell,k}, F_{\ell,k})$ such that

$$\|\varepsilon_A^k - \varepsilon_B^k\|_\infty \leq c_{\ell,k} \operatorname{dist}_\infty(\varepsilon_A^k, B_{\ell,k}).$$

Let $\varepsilon^k \in B_{\ell,k}$ and $\varepsilon^\ell \in \mathbb{R}^{N_\ell}$: $\varepsilon^k = P_\ell^k \varepsilon^\ell$. Then, using eq. (8) and eq. (35) we have

$$\|P_\ell^k \varepsilon^\ell - \varepsilon_A^k\|_\infty \leq d_1^{-1} \|P_k^L (P_\ell^k \varepsilon^\ell - \varepsilon_A^k)\|_\infty = d_1^{-1} \|z^{L,\ell} + P_\ell^L \varepsilon^\ell - z^{L,k+1}\|_\infty,$$

thus

$$\begin{aligned} \operatorname{dist}_\infty(\varepsilon_A^k, B_{\ell,k}) &\leq d_1^{-1} \inf \{ \|z^{L,\ell} + P_\ell^L \varepsilon^\ell - z^{L,k+1}\|_\infty : P_\ell^k \varepsilon^\ell \in B_{k,\ell} \} \\ &= d_1^{-1} \operatorname{dist}(z^{L,k+1}, \Xi_\ell \cap D). \end{aligned}$$

Therefore

$$\|z^{L,k+1} - z^{L,\ell+1}\|_\infty \leq d_2 \|\varepsilon_A^k - \varepsilon_B^k\|_\infty \leq c_{\ell,k} \frac{d_2}{d_1} \operatorname{dist}(z^{L,k+1}, \Xi_\ell \cap D). \quad (36)$$

To see that $c_{\ell,k}$ on the right hand side can be substituted by a universal constant, independent of ℓ, k , we proceed as follows: Recall that, from lemma 2, $c_{\ell,k} = c(A_{\ell,k}, F_{\ell,k}) = \sqrt{\rho_{\max}^{l,k} / \rho_{\min}^{l,k}}$ with

$$\rho_{\min}^{l,k} = \min_{\xi^k \in A_{\ell,k}} \min_{\varepsilon^k \neq 0} \frac{(\varepsilon^k)^T \nabla^2 F_{\ell,k}(\xi^k) \varepsilon^k}{\|\varepsilon^k\|_\infty^2}, \quad \rho_{\max}^{l,k} = \max_{\xi^k \in A_{\ell,k}} \max_{\varepsilon^k \neq 0} \frac{(\varepsilon^k)^T \nabla^2 F_{\ell,k}(\xi^k) \varepsilon^k}{\|\varepsilon^k\|_\infty^2}.$$

Taking into account that $\forall \xi^k \in \mathbb{R}^{N_k}$

$$\nabla^2 F_{\ell,k}(\xi^k) = (P_k^L)^T \nabla^2 F(z^k) P_k^L, \quad z^k = z^{L,\ell} + P_k^L \xi^k,$$

and recalling that eq. (8) implies $P_k^L \varepsilon^k \neq 0$ when $\varepsilon_k \neq 0$, we can write

$$\begin{aligned} \frac{(\varepsilon^k)^T \nabla^2 F_{\ell,k}(\xi^k) \varepsilon^k}{\|\varepsilon^k\|_\infty^2} &= \frac{(P_k^L \varepsilon^k)^T \nabla^2 F(z^k) (P_k^L \varepsilon^k)}{\|P_k^L \varepsilon^k\|_\infty^2} \frac{\|P_k^L \varepsilon^k\|_\infty^2}{\|\varepsilon^k\|_\infty^2} \\ &\geq \frac{(P_k^L \varepsilon^k)^T \nabla^2 F(z^k) (P_k^L \varepsilon^k)}{\|P_k^L \varepsilon^k\|_\infty^2} d_1^2 \geq \min_{\varepsilon^L \neq 0} \frac{(\varepsilon^L)^T \nabla^2 F(z^k) \varepsilon^L}{\|\varepsilon^L\|_\infty^2} d_1^2. \end{aligned}$$

Since $\xi^k \in A_{\ell,k} \Rightarrow z^k = z^{L,\ell} + P_k^L \xi^k \in \Xi_k \cap D$, we have that

$$\rho_{\min}^{l,k} \geq \rho_{\min}(F, D) d_1^2, \quad \text{with} \quad \rho_{\min}(F, D) := \min_{z \in D} \min_{\varepsilon^L \neq 0} \frac{(\varepsilon^L)^T \nabla^2 F(z) \varepsilon^L}{\|\varepsilon^L\|_\infty^2}, \quad (37)$$

proceeding analogously with the upper bounds, we have that

$$\rho_{\max}^{l,k} \leq \rho_{\max}(F, D)d_2^2, \quad \text{with} \quad \rho_{\max}(F, D) := \max_{z \in D} \max_{\varepsilon^L \neq 0} \frac{(\varepsilon^L)^T \nabla^2 F(z) \varepsilon^L}{\|\varepsilon^L\|_\infty^2}. \quad (38)$$

Thus, we obtain eq. (33) with

$$C = C(F, D, \mathcal{P}) := \sqrt{\frac{\rho_{\max}(F, D) d_2^2}{\rho_{\min}(F, D) d_1^2}}.$$

□

This result allows us to relate the difference between sub-optimal solutions to the size of certain detail coefficients.

Theorem 1. *Let $F \in \mathcal{C}^2(\mathbb{R}^{N_L}, \mathbb{R})$ and \mathcal{P} as in proposition 3. Then, for any pair of indices ℓ, k , $0 \leq \ell \leq k < L$ there exists $C > 0$, independent of ℓ, k , such that*

$$\|z^{L,k+1} - z^{L,\ell+1}\|_\infty \leq C \|(d^\ell(z^{L,k+1} - z^{L,0}), \dots, d^{k-1}(z^{L,k+1} - z^{L,0}))\|_\infty. \quad (39)$$

Proof. From eq. (26) and eq. (27), we can write

$$M_{\ell,L} z^{L,\ell+1} = (z^\ell, \bar{d}^\ell, \dots, \bar{d}^{L-1}), \quad M_{k,L} z^{L,k+1} = (z^k, \bar{d}^k, \dots, \bar{d}^{L-1}),$$

with $z^m := z_*^m + \varepsilon_*^m \in \mathbb{R}^{N_m}$, $m = k, \ell$ and $\bar{d}^j = d^j(z^{L,0})$. Since $\ell \leq k$, by eq. (5),

$$M_{\ell,L} z^{L,k+1} = (M_{\ell,k} z^k, \bar{d}^k, \dots, \bar{d}^{L-1}) = (x^\ell, \hat{d}^\ell, \dots, \hat{d}^{k-1}, \bar{d}^k, \dots, \bar{d}^{L-1}),$$

with $x^\ell \in \mathbb{R}^{N_\ell}$, $\hat{d}^j = d^j(z^{L,k+1})$ (see section 2.1). Then,

$$M_\ell^L (z^{L,k+1} - z^{L,\ell+1}) = (x^\ell - z^\ell, \hat{d}^\ell - \bar{d}^\ell, \dots, \hat{d}^{k-1} - \bar{d}^{k-1}, 0, \dots, 0).$$

Thus, $w^{\ell,k} := z^{L,\ell+1} + P_\ell^L (x^\ell - z^\ell) \in \Xi_\ell$ satisfies

$$M_{\ell,L} (z^{L,k+1} - w^{\ell,k}) = (0, \hat{d}^\ell - \bar{d}^\ell, \dots, \hat{d}^{k-1} - \bar{d}^{k-1}, 0, \dots, 0). \quad (40)$$

Let D be a compact set containing all the iterates $\{z^{L,m}\}_{m=0}^{L+1}$ and all the points $w^{\ell,k}$, $\forall \ell, k : 0 \leq \ell \leq k < L$. Applying proposition 3 $\exists C = C(F, D, \mathcal{P})$ such that

$$\|z^{L,k+1} - z^{L,\ell+1}\|_\infty \leq C \text{dist}(z^{L,k+1}, \Xi_\ell \cap D) \leq C \|z^{L,k+1} - w^{\ell,k}\|_\infty.$$

Since $\|z^{L,k+1} - w^{\ell,k}\|_\infty = \|M_{\ell,k}^{-1} M_{\ell,L} (z^{L,k+1} - w^{\ell,k})\|_\infty$, by eq. (40) and eq. (7), we have

$$\begin{aligned} \|z^{L,k+1} - z^{L,\ell+1}\|_\infty &\leq C \left\| M_{\ell,L}^{-1} \left(0, \hat{d}^\ell - \bar{d}^\ell, \dots, \hat{d}^{k-1} - \bar{d}^{k-1}, 0, \dots, 0 \right) \right\|_\infty \\ &\leq C \tilde{C} \|(d^\ell(z^{L,k+1} - z^{L,0}), \dots, d^{k-1}(z^{L,k+1} - z^{L,0}))\|_\infty, \end{aligned}$$

since $\hat{d}^m - \bar{d}^m = d^m(z^{L,k+1} - z^{L,0})$, by the linearity of the MR transformations. □

Under smoothness assumptions, the decay of the detail coefficients is related to the approximation properties of the prediction scheme, which allows to obtain quantitative estimates for the distance between sub-optimal solutions. .

Corollary 1. Let $F \in C^2(\mathbb{R}^{N_L}, \mathbb{R})$ as in proposition 3, and $\mathcal{P} = \{P_k^{k+1}\}_{k \geq 0}$ the sequence of interpolatory prediction operators given in section 2.1. If the initial guess $\bar{z} = z^{L,0}$ and $z_{\min} = \arg \min\{F(z), z \in \mathbb{R}^{N_L}\}$ can be associated to the point evaluations on \mathcal{G}^L of sufficiently smooth functions, then for $0 \leq \ell < L$,

1. $\|z_{\min} - z^{L,\ell+1}\|_{\infty} = O(h_{\ell+1}^{n+1})$,
2. $\|z^{L,\ell+1} - z^{L,\ell}\|_{\infty} = O(h_{\ell}^{n+1})$,
3. $\|\varepsilon_*^{\ell}\|_{\infty} = O(h_{\ell}^{n+1})$.

Proof. If $z_{\min} - \bar{z}$ can be considered as point evaluations of a sufficiently smooth function, we have that $\|d^j(z_{\min} - \bar{z})\|_{\infty} = O(h_{j+1}^{n+1})$, $0 \leq j < L$. To prove item 1 we take $k = L$ in theorem 1. Since $z^{L,L+1} = z_{\min}$, $\bar{z} = z^{L,0}$, we have

$$\|z_{\min} - z^{L,\ell+1}\|_{\infty} \leq C\|(d^{\ell}(z_{\min} - \bar{z}), \dots, d^{L-1}(z_{\min} - \bar{z}))\|_{\infty} = O(h_{\ell+1}^{n+1}).$$

item 2 and item 3 follow from the previous result, since

$$\|z^{L,\ell} - z^{L,\ell+1}\|_{\infty} \leq \|z_{\min} - z^{L,\ell}\|_{\infty} + \|z_{\min} - z^{L,\ell+1}\|_{\infty}$$

and $z^{L,\ell+1} - z^{L,\ell} = P_{\ell}^L \varepsilon_*^{\ell}$, hence, by eq. (8),

$$\|\varepsilon_*^{\ell}\|_{\infty} \leq d_1^{-1} \|P_{\ell}^L \varepsilon_*^{\ell}\|_{\infty} = d_1^{-1} \|z^{L,\ell+1} - z^{L,\ell}\|_{\infty}.$$

□

We summarize the results shown in this section as follows: For (suitable) convex optimization problems, the distance between sub-optimal solutions is related to the size of certain detail coefficients. Provided that both the solution and the initial guess are *smooth*, the ∞ -distance between consecutive sub-optimal solutions decreases when climbing up the MR ladder (at a rate which depends on the properties of the prediction operators). In this case, even though the auxiliary minimization problems eq. (24) involve an increasing number of degrees of freedom when the resolution level increases, it seems reasonable to assume that they will be *efficiently* solved by the given optimization technique, due to the fact that the initial guess and the solution of each auxiliary problem are increasingly *closer*.

Our theoretical results are numerically validated in the next section.

4 Numerical Experiments

The common setting for our numerical experiments is as follows: We seek to solve eq. (1) by embedding the problem into an appropriate interpolatory MR Framework and using the MR/OPT strategy with a given minimization tool (\mathcal{D}) and an initial guess, \bar{z} , which we assume supplied by the end-user. We recall the following two important points in our approach:

1. The solution of the *auxiliary minimization problems* eq. (24) can be carried out using only the objective function F (as a black box routine). Moreover, in practice only the prediction rules of the MR transformation are really required for the application of our algorithm.
2. The chosen optimizer, \mathcal{D} , is also a black-box routine in the algorithm.

In this paper we shall consider two different optimization tools from MATLAB: `fminunc`, a *steepest descent method* which requires a gradient estimation, and the general purpose optimization tool `patternsearch`, which is a *coordinate search method*. When using them as black-box tool, a series of parameters need to be specified. We set the running parameters seeking to stop \mathcal{D} when the max-norm of the difference between two consecutive iterates within the call falls below a specified tolerance ($tol_{\mathcal{D}}$)⁷.

In addition, it seems reasonable to consider

$$\|z^{L,k+1} - z^{L,k}\| \leq tol_M \quad (41)$$

as a suitable stopping criteria for the MR/OPT strategy, in order to avoid unnecessary calls to the optimizer. In our numerical experiments we always choose $tol_M = tol_{\mathcal{D}}$.

The tests considered in the following subsections are taken from the specialized literature. In all the cases considered, the MR/OPT strategy leads to a *more efficient* computation than the direct use of \mathcal{D} to solve eq. (1). To measure the performance of the MR/OPT strategy, we have considered, as in [23], the total number of evaluations of the objective function F , since often the remaining operations may have a negligible cost compared to that. In addition, we also examine the ratio between the number of functional evaluations required to solve each k -th auxiliary problem versus its number of degrees of freedom, because it also provides very valuable information on the behavior of the strategy.

All the computations have been done with MATLAB R2020b on a MacBook Air with a 1,8 GHz Intel Core i5 double core processor and a 8 GB 1600 MHz DDR3 memory.

4.1 Quadratic Optimization Problems

Boundary Value Problems (BVP) in ordinary and partial differential equations are a common source of large scale optimization problems. In many cases, the discrete setting corresponds to a quadratic minimization problem of the type considered in proposition 1. Here, we shall consider 1D and 2D BVP with smooth solutions in order to check numerically the theoretical results stated in the previous section.

We consider first the 1D BVP (from [30]),

$$\begin{cases} -u''(t) + 2u(t) = f(t), & t \in (0, 1) \\ u(0) = u(1) = 0. \end{cases} \quad (42)$$

where $f(t) := 10^6 t(1-t)(t-1/2)(t-1/4)(3/4-t)$. Using the standard centered second order discretization for u'' on the uniform grid $\mathcal{G} := (i/J)_{i=0}^J$ leads to the linear system

$$(-z_{i-1} + 2z_i - z_{i+1})J^2 + 2z_i = f(i/J), \quad i = 1, 2, \dots, J-1,$$

for the unknown values $z_i = u(i/J) + O(h^2)$, $h = 1/J$, $1 \leq i \leq J-1$ ($z_0 = z_J = 0$ because of the boundary conditions). In practice, J is *sufficiently large* so that the (discrete) solution of the linear system is *sufficiently close* to the true solution of the ODE, according to the end-user.

The coefficient matrix for the system $A \in \mathbb{R}^{(J-1) \times (J-1)}$, is banded, symmetric and definite positive, hence the solution can be found by solving a quadratic minimization problem of the type stated in proposition 1. We compute the solution of this minimization problem using the MR/OPT

⁷In our implementation the running parameters (consult its documentation for further information) are `TolX` = $tol_{\mathcal{D}}$, `TolFun`=0 and `MaxFunEvals`=`MaxIter`=Inf. For `fminunc` we additionally established `OptimalityTolerance`=0, `Algorithm`=quasi-newton, `FinDiffRelStep`=1e-13 and `FiniteDifferenceType`=central.

strategy in combination with the 1D Interpolatory MR setting described in section 2.1. For this, we consider $J = J_L$, $\mathcal{G} = \mathcal{G}_L$ as the finest mesh in a ladder of nested uniform grids on $[0, 1]$ of the form $\mathcal{G}_k = (i/J_k)_{i=0}^{J_k}$, $J_k = J_{k+1}/2$, $0 \leq k < L$. Hence, the discrete spaces in the corresponding 2D-interpolatory MR setting have dimension $(J_k + 1)$. In our computations, we take $J_L = 128 = 2^7$, $L = 5$ (i.e. $J_0 = 4$), $tol_{\mathcal{D}} = 10^{-6} = tol_M$.

Considering the zero vector as initial data, we comply with the boundary conditions, i.e. $\bar{z} = z^{L,0} = \bar{0} \in \mathbb{R}^{N^L}$. At each resolution level we enforce $\varepsilon_0^k = 0 = \varepsilon_{J_k}^k$ when applying the prediction operators and, as a result, the sub-optimal solutions associated to the auxiliary optimization problems naturally satisfy the boundary conditions. In fig. 1, we display $z^{L,k+1}$ for $k = 0, 1, 2$ and the different prediction operators in section 2.1. For $n = 1$, the sub-optimal solution is a piecewise linear function, while for $n = 3, 5$ we can clearly observe that the sub-optimal solutions are *smoother*⁸. The plots shown correspond to $\mathcal{D} = \text{fminunc}$, but are indistinguishable from those obtained with $\mathcal{D} = \text{patternsearch}$.

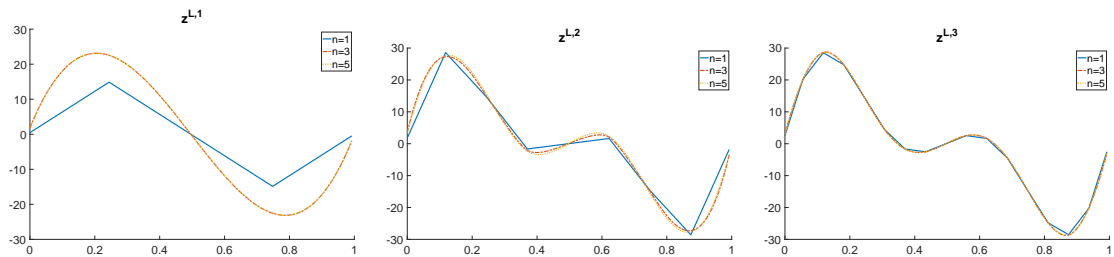


Figure 1: 1D BVP ($\mathcal{D} = \text{fminunc}$). The sub-optimal solutions $z^{L,1}, z^{L,2}, z^{L,3}$, from left to right, for $n = 1, 3, 5$.

In fig. 2, we clearly observe that the decay rates of (the max-norm of) the difference between the sub-optimal solutions and z_{\min} ⁹, and the difference between two consecutive sub-optimal solutions, depend on the prediction scheme, but not on the optimization tool, just as predicted by our theoretical results. The table below the plots, shows a numerical estimation of the decay rate corresponding to the values $\|z^{L,k+1} - z^{L,k}\|_{\infty}$ obtained when using **fminunc** (the results for **patternsearch** are similar and are not shown), computed as

$$r = \log_2 \frac{\|z^{L,k} - z^{L,k-1}\|_{\infty}}{\|z^{L,k+1} - z^{L,k}\|_{\infty}}. \quad (43)$$

Since the optimization problem fulfills all the hypothesis stated in Theorem 1 and Corollary 1, the numerical decay rates coincide with the expected decay rates of the detail coefficients eq. (17) for each choice of the prediction scheme.

In fig. 3 we examine the *efficiency* of the MR/OPT strategy. The table below the plots clearly shows that the MR/OPT strategy leads to a significant improvement in efficiency compared to the direct application of the optimization tool. Since **fminunc** is a much more *efficient* optimizer for this type of problems, its use leads to a smaller number of functional evaluations, both when applied directly or when used in the MR/OPT strategy. It is worth observing that the MR/OPT strategy leads to large improvements in efficiency: the total number of evaluations carried out with the MR/OPT for $n = 5$, is less than 18% for **fminunc** and 0.7% for **patternsearch**.

⁸These facts are related to the properties of the prediction scheme.

⁹Computed with `A\b` of MATLAB.

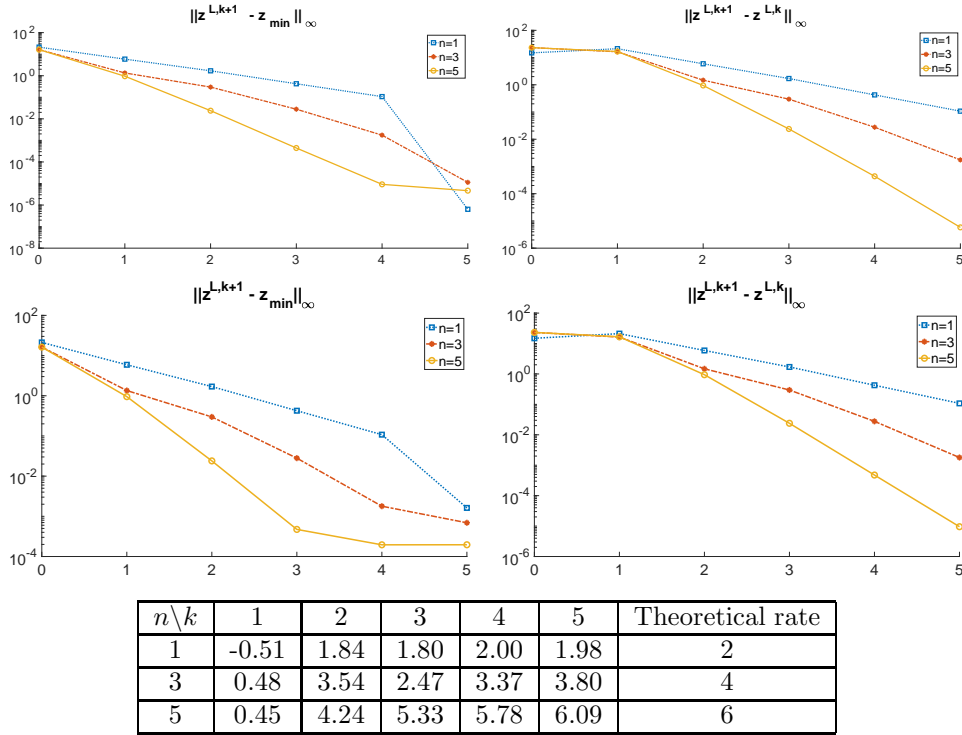


Figure 2: 1D BVP. $tol_{\mathcal{D}} = tol_M = 10^{-6}$. Horizontal axis, k (resolution level). Top row, $\mathcal{D} = \text{fminunc}$; Bottom row, $\mathcal{D} = \text{patternsearch}$. Left column, ∞ -distance between $z^{L,k+1}$ and z_{\min} . Right column, ∞ -distance between consecutive sub-optimal solutions. Table, numerical estimation of r in eq. (43), for $\mathcal{D} = \text{fminunc}$.

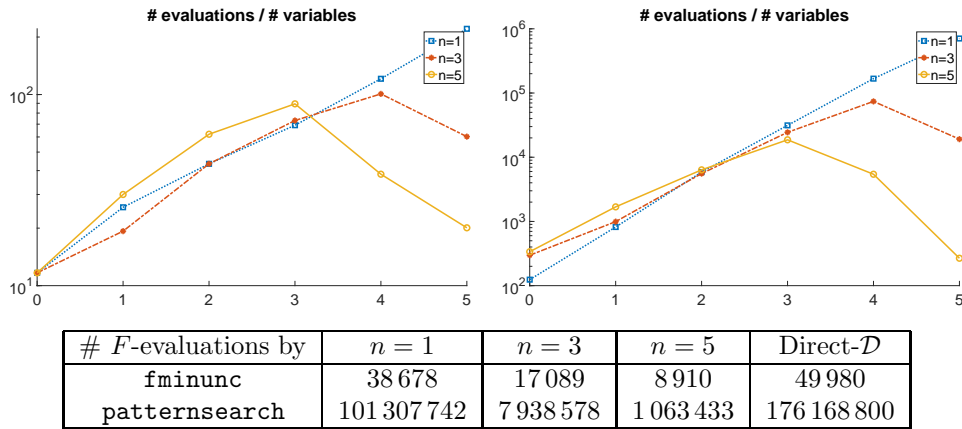


Figure 3: 1D BVP, as in fig. 2. Ratio between the number of functional evaluations and the number of degrees of freedom involved in the solution of the k -th auxiliary problem, versus k . Left: $\mathcal{D} = \text{fminunc}$; Right: $\mathcal{D} = \text{patternsearch}$. Table: Total number of functional evaluations required to find $z^{L,L+1}$ in each case.

We can see in the plots of fig. 3 that the number of functional evaluations over the number of degrees of freedom increases in a similar way for $n = 1, 3, 5$ for the lower resolution levels, but this ratio decays at the higher resolution levels for $n = 3, 5$. A plausible explanation is that the distance between the initial guess and the solution of the k -th auxiliary problem decreases with n and k , as specified in corollary 1, hence the corresponding optimization problems can be solved in less iterations. Thus, the efficiency improves with the approximation order of the prediction scheme used.

Notice, however, that even in the ‘least efficient’ case ($n = 1$), the MR/OPT reaches the desired solution more efficiently than with the direct optimizer, *without any additional effort by the end-user*.

Our second test case is the P2D in [22],

$$\begin{aligned} -(u_{xx}(x, y) + u_{yy}(x, y)) &= f(x, y), & (x, y) \in \text{int}(\Omega), \\ u(x, y) &= 0, & (x, y) \in \partial\Omega, \end{aligned} \tag{44}$$

$\Omega = [0, 1] \times [0, 1]$, $\partial\Omega$ and $\text{int}(\Omega)$ denoting the boundary and the interior of Ω , but with a smooth, non-polynomial right hand side, $f(x, y) = \sin(4\pi x(1-x)y(1-y))$.

A standard discretization of eq. (44) (using the classical 5-point Laplacian, see [22]), on a uniform grid $\mathcal{G} := (i/J, j/J)_{i,j=0}^J$, leads to a system of equations that can be written in matrix form as $Az = b$, $z(i, j) = u(i/J, j/J) + O(h^2)$, where $h = 1/J$ is the uniform mesh spacing of \mathcal{G} and A is symmetric and definite positive. As in the 1D case, finding z may be formulated as a quadratic, convex, minimization problem, but in the 2D case there are $N = (J-1)^2$ degrees of freedom, so that solving the associated minimization problem is a much more demanding task, for the same accuracy in the resulting approximation.

We solve the minimization problem using the MR/OPT strategy in combination with the 2D-tensor product interpolatory MR described in section 2.1. For this, we consider $J = J_L$, $\mathcal{G} = \mathcal{G}_L$ as the finest mesh in a ladder of nested uniform grids on Ω of the form $\mathcal{G}_k = (i/J_k, j/J_k)_{i,j=0}^{J_k}$, $J_k = J_{k+1}/2$, $0 \leq k < L$. The discrete spaces in the corresponding 2D-interpolatory MR setting have dimension $(J_k + 1)^2$. In our computations, we take zero initial data, $J_L = 128$, $L = 5$, $tol_M = tol_{\mathcal{D}} = 10^{-7}$ and $\mathcal{D} = \text{fminunc}$.

fig. 4 shows several plots analogous to those in fig. 2-fig. 3, where we observe the same behavior as in the 1D case: The actual errors between the auxiliary solutions and the true solution decrease, and also the efficiency of the MR/OPT strategy increases, with the approximation order of the prediction scheme. The decay rate of the max-norm errors between the sub-optimal solutions and the true solution, and also between successive sub-optimal solutions, coincides with the order of approximation of the prediction operators (see table 1), which is consistent with corollary 1.

It is worth noticing that in this test case the max-norm of the difference between sub-optimal solutions falls below $tol_M = tol_{\mathcal{D}}$ at $k = 3$ for $n = 5$, and $k = 4$ for $n = 3$, which makes the MR/OPT strategy stop¹⁰. We also remark the very large increment in efficiency obtained for $n = 3, 5$, compared to $n = 1$, which is probably due to the smoothness of the solution. For $n = 5$, the solution has been obtained with only 0.1% of the functional evaluations required by the direct use of `fminunc`.

4.2 Non-quadratic problems

In this subsection we shall consider: a convex, but non-quadratic, minimization problem and a non-convex problem, in order to evaluate the performance of our MR/OPT strategy, in more general situations

¹⁰For larger values of $tol_{\mathcal{D}} = tol_M$, the strategy stop even at lower resolution levels.

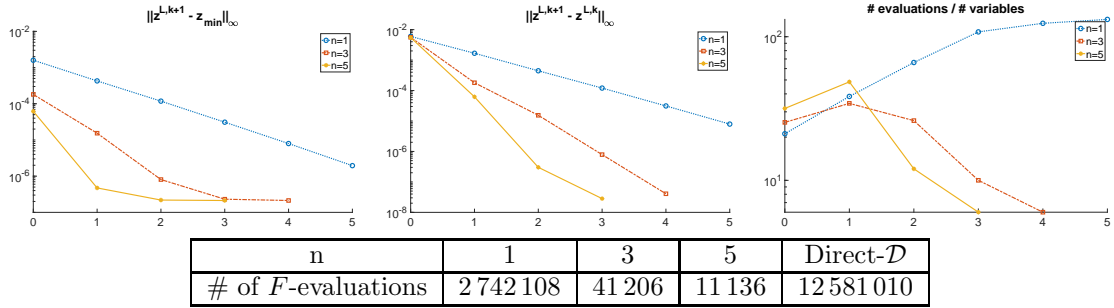


Figure 4: 2D Poisson problem eq. (44), $L = 5$, $tol_M = tol_{\mathcal{D}} = 10^{-7}$. \mathcal{D} is `fminunc`.

$n \setminus k$	1	2	3	4	5	Theoretical rate
1	1.84	1.91	1.89	1.95	1.98	2
3	5.27	3.36	4.14	4.27	-	4
5	6.72	7.59	3.62	-	-	6

Table 1: Test-case: 2D Poisson problem. Decay rate eq. (43) for the data in fig. 4.

We consider first the MINS problem in [22], which arises from a discretization of the following minimal surface problem

$$\min_u \int_{\Omega} \sqrt{1 + \|\nabla u(x, y)\|_2^2} d(x, y), \quad (45)$$

with the boundary conditions

$$u_0(x, y) = \begin{cases} x(1-x), & \text{if } y \in \{0, 1\}, \\ 0, & \text{otherwise.} \end{cases}$$

Its solution is approximated in [22] by the solution of the minimization problem that results from considering as objective function

$$F(z) := \frac{1}{2J^2} \sum_{i,j=0}^{J-1} \sqrt{1 + a^2 + b^2} + \sqrt{1 + c^2 + d^2},$$

with

$$\begin{aligned} a &= J(z_{i,j+1} - z_{i,j}), & b &= J(z_{i+1,j+1} - z_{i,j+1}), \\ c &= J(z_{i+1,j+1} - z_{i+1,j}), & d &= J(z_{i+1,j} - z_{i,j}). \end{aligned}$$

We use the interpolatory 2D framework and the MR/OPT strategy to solve this nonlinear, convex, optimization problem, with $J_L = 128$, $L = 5$, $tol_M = tol_{\mathcal{D}} = 10^{-6}$ and $z_{i,j}^{L,0} = \frac{i}{J}(1 - \frac{j}{J})$, $i, j \in \{0, 1, \dots, J\}$, which complies with the specified boundary conditions. The solution obtained with MR/OPT and $\mathcal{D}=\text{fminunc}$ with the above parameters is represented in fig. 7-left.

In this case, we do not know the exact solution and in fig. 5-left we only plot the max-norm of the difference between sub-optimal solutions. The observed decay rate is $r \approx 2$, for all prediction schemes. To explain this apparent contradiction with the results in corollary 1, we carry out a numerical inspection of the derivatives of the solution shown in fig. 7-left. We observe large spikes

in third order derivatives at the four corners of the unit square, which is an indication that the obtained discrete data can only be associated to a \mathcal{C}^2 function. Hence, the observed decay rate is, in fact, the one predicted by the theoretical result in corollary 1 since, in this case, the interpolation error corresponding to an n -th degree polynomial ($n \geq 1$) is only $O(h^2)$, with h the distance between the points in the grid.

The plot in fig. 5-right shows, again, the increase in efficiency of the MR/OPT strategy for $n = 3, 5$, which we assume to be related to the fact that the errors between consecutive sub-optimal solutions are smaller than for $n = 1$, hence the corresponding auxiliary optimization problems require less iterations. For $n = 5$, the solution of the original optimization problem, shown in fig. 7-right, is obtained with less than 2 % of the total number of evaluations of F , with respect to the direct application of \mathcal{D} .

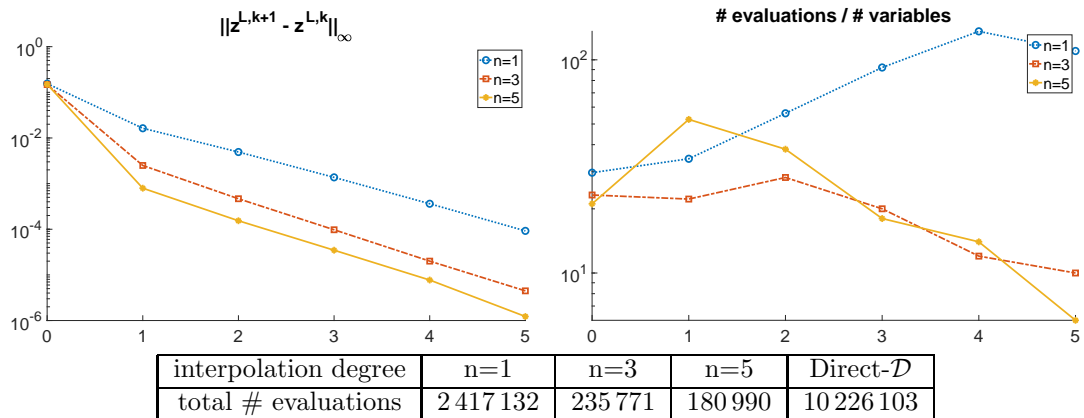


Figure 5: Minimal surface problem. $L = 5$, $tol_M = tol_{\mathcal{D}} = 10^{-6}$ and \mathcal{D} is `fminunc`.

Our last test concerns a nonlinear non-convex optimization problem from [22, section 5.1.4]: the MOREBV problem, which is obtained from a discretization on a uniform grid on $\Omega = [0, 1] \times [0, 1]$ of the following BVP

$$\begin{aligned} -(u_{xx}(x, y) + u_{yy}(x, y)) + \frac{1}{2}(u(x, y) + x + y + 1)^3 &= 0, & (x, y) \in \text{int}(\Omega), \\ u(x, y) &= 0, & (x, y) \in \partial\Omega. \end{aligned} \quad (46)$$

Using the classical 5-point discretization of the Laplacian, the resulting system of nonlinear equations can be rewritten as a nonlinear least-squares problem with a non-convex objective function given by the expression (see [22] and references therein). The theoretical results of section 3.1 do not apply in this case.

$$\begin{aligned} F(z) := \sum_{i,j=1}^{J-1} & \left((4z_{i,j} - z_{i-1,j} - z_{i+1,j} - z_{i,j-1} - z_{i,j+1}) \right. \\ & \left. + \frac{1}{2J^2} (z_{i,j} + i/J + j/J + 1)^3 \right)^2. \end{aligned} \quad (47)$$

We solve this problem by using the MR/OPT strategy within the 2D interpolatory MR framework used in the previous two test cases. As before, setting $\bar{z} = \vec{0}$ leads to a sequence of sub-optimal solutions satisfying the boundary conditions. The solution obtained with the same parameters as in the previous test case ($n = 5$) is shown in fig. 7-right.

In fig. 6 we show the results obtained for this test case. The left plot in this figure shows that when taking $n = 1$ the distance between consecutive sub-optimal solutions does not decay¹¹, but it does decrease for $n = 3, 5$ (at a rate $r \approx 2$). As a consequence, the number of calls to the objective function increases dramatically for $n = 1$, while it remains moderate for $n = 3, 5$. More research is required to explain the behavior of the MR/OPT strategy for this non-convex optimization problem, for which no theoretical results are provided in this paper. We have observed that, as in the MINS problem, certain third order finite differences of $z^{L,L+1}$ also exhibit peaks in the corners of Ω . We do remark that the solution corresponding at $n = 5$ has been obtained with less than 0.3% of the total number of functional evaluations than for $n = 1$ (which is, at least, less than 69% of the total number of evaluations for the direct use of \mathcal{D}).

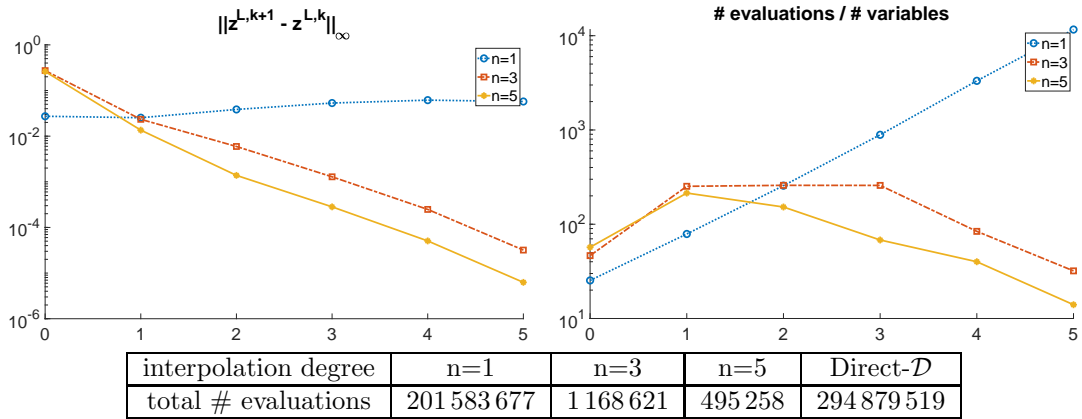


Figure 6: MOREBV problem. $L = 7$, $tol_M = tol_{\mathcal{D}} = 10^{-6}$ and \mathcal{D} is `fminunc`.

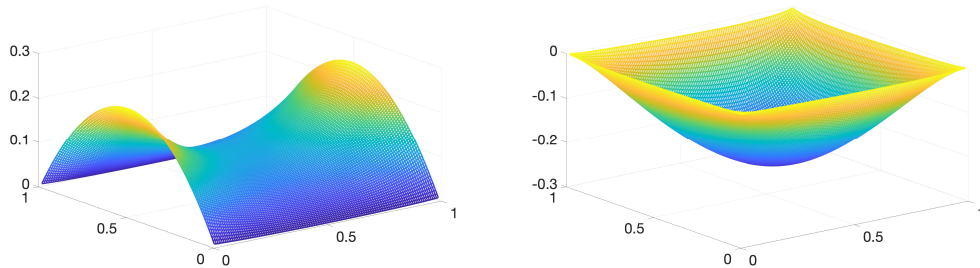


Figure 7: The computed solution, $z^{L,L+1}$, of the minimal surface (left) and the MOREBV (right) problems taking $n = 5$.

5 Conclusions And Perspectives

We have described and analyzed a multilevel strategy (MR/OPT) which can be used to reduce the cost of solving large scale optimization problems. MR/OPT uses Harten's MRF to define a hierarchy

¹¹The set of sub-optimal solutions can be found in the Appendix.

of auxiliary problems that provide a sequence of *sub-optimal solutions*, one at each resolution level, so that at the last step the full (large-scale) optimization problem is solved, but with an initial guess that is much closer to the desired solution than the original initial guess (which is assumed to be provided by the end-user).

The solutions of the auxiliary problems depend on the prediction operators of the chosen MRF. The results in this paper clearly demonstrate that the accuracy of the prediction scheme plays a significant role in the overall performance of the MR/OPT strategy, when the initial guess and the solution can be interpreted as point-value discretizations of sufficiently smooth functions.

Harten's MRF provides a flexible and versatile multilevel structure that allows to consider both the optimization tool and the objective function eq. (1) as black boxes, which is an important asset in engineering applications. If an optimization problem such a eq. (1) can be solved with a specific optimization tool, \mathcal{D} , MR/OPT will reduce the cost of finding its solution. For convex optimization problems, we have presented several theoretical results on the properties and the performance of the MR/OPT strategy, which have been numerically validated in a series of examples from the specialized literature. More analytic work is necessary in order to determine the properties of the MR/OPT strategy in more general situations, as well as the influence of the underlying minimization code or the specification of constraints.

The strategy can be improved in various ways, that we intend to investigate in future papers. In particular, it might be advantageous to consider a level-dependent tolerance criterion for the optimizer \mathcal{D} : large tolerances in coarse levels and small ones in fine levels. Following this idea, to consider different optimizers might also be profitable: e.g. global searchers in the first levels and, later, fast/local optimizers. Another line of research concerns the use of nonlinear reconstruction techniques instead of the linear ones used in this paper, since they might be more efficient in problems where the solution presents discontinuities or it is important to preserve specific features of the solution, such as monotonicity or convexity.

References

- [1] Remi Abgrall, Pietro Marco Congedo, and Gianluca Geraci. A one-time truncate and encode multiresolution stochastic framework. *Journal of Computational Physics*, 257:19–56, 2014.
- [2] Francesc Aràndiga and Rosa Donat. Nonlinear multiscale decompositions: the approach of A. Harten. *Numerical Algorithms*, 23(2-3):175–216, 2000.
- [3] Francesc Aràndiga, Rosa Donat, and Ami Harten. Multiresolution based on weighted averages of the hat function i: Linear reconstruction techniques. *SIAM Journal on Numerical Analysis*, 36(1):160–203, 1998.
- [4] Francesc Aràndiga, Rosa Donat, and Ami Harten. Multiresolution based on weighted averages of the hat function i: Linear reconstruction techniques. *SIAM Journal on Numerical Analysis*, 36(1):160–203, 1998.
- [5] Francesc Aràndiga, Pep Mulet, and Vicent Renau. Lossless and near-lossless image compression based on multiresolution analysis. *Journal of Computational and Applied Mathematics*, 242:70–81, 2013.
- [6] Barna L. Bihari and Ami Harten. Multiresolution schemes for the numerical solution of 2-d conservation laws i. *SIAM J. Sci. Comput.*, 18:315–354, 1997.

- [7] Barna L Bihari and Donald Schwendeman. Multiresolution schemes for the reactive euler equations. *Journal of Computational Physics*, 154(1):197–230, 1999.
- [8] Achi Brandt. Multi-level adaptive solutions to boundary-value problems. *Mathematics of computation*, 31(138):333–390, 1977.
- [9] WL Briggs. *A Multigrid Tutorial*. 1987.
- [10] Raymond H Chan and Ke Chen. A multilevel algorithm for simultaneously denoising and deblurring images. *SIAM Journal on Scientific Computing*, 32(2):1043–1063, 2010.
- [11] Tony F Chan and Ke Chen. An optimization-based multilevel algorithm for total variation image denoising. *Multiscale Modeling & Simulation*, 5(2):615–645, 2006.
- [12] Cheng Chen, Zaiwen Wen, and Ya-xiang Yuan. A general two-level subspace method for non-linear optimization. *Journal of Computational Mathematics*, 36(6), 2018.
- [13] Guillaume Chiavassa and Rosa Donat. Point value multiscale algorithms for 2d compressible flows. *SIAM Journal on Scientific Computing*, 23(3):805–823, 2001.
- [14] Albert Cohen, Sidi Kaber, Siegfried Müller, and Marie Postel. Fully adaptive multiresolution finite volume schemes for conservation laws. *Mathematics of Computation*, 72(241):183–225, 2003.
- [15] B Colson, M Porcelli, and Ph L Toint. Aircraft fuselage sizing with multilevel optimization. 2013.
- [16] Johan M De Villiers, Karin M Goosen, and Ben M Herbst. Dubuc–deslauriers subdivision for finite sequences and interpolation wavelets on an interval. *SIAM Journal on Mathematical analysis*, 35(2):423–452, 2003.
- [17] Johan M De Villiers, Karin M Goosen, and Ben M Herbst. Dubuc–deslauriers subdivision for finite sequences and interpolation wavelets on an interval. *SIAM Journal on Mathematical analysis*, 35(2):423–452, 2003.
- [18] Rosa Donat and Sergio López-Ureña. High-accuracy approximation of piecewise smooth functions using the truncation and encode approach. *Applied Mathematics and Nonlinear Sciences*, 2(2):367–384, 2017.
- [19] Rosa Donat, Sergio López-Ureña, and Marc Menec. A novel multi-scale strategy for multi-parametric optimization. In *European Consortium for Mathematics in Industry*, pages 593–600. Springer, 2016.
- [20] Nira Dyn. Subdivision schemes in cagd. *Advances in numerical analysis*, 2:36–104, 1992.
- [21] Nira Dyn. Subdivision schemes in cagd. *Advances in numerical analysis*, 2:36–104, 1992.
- [22] Emanuele Frandi and Alessandra Papini. Coordinate search algorithms in multilevel optimization. *Optimization Methods and Software*, 29(5):1020–1041, 2014.
- [23] Emanuele Frandi and Alessandra Papini. Improving direct search algorithms by multilevel optimization techniques. *Optimization Methods and Software*, 30(5):1077–1094, 2015.

- [24] Serge Gratton, Annick Sartenaer, and Philippe L Toint. Recursive trust-region methods for multiscale nonlinear optimization. *SIAM Journal on Optimization*, 19(1):414–444, 2008.
- [25] Wolfgang Hackbusch. Convergence of multigrid iterations applied to difference equations. *Mathematics of Computation*, 34(150):425–440, 1980.
- [26] Xiacong Han and David W Zingg. An adaptive geometry parametrization for aerodynamic shape optimization. *Optimization and Engineering*, 15(1):69–91, 2014.
- [27] Ami Harten. Multiresolution representation of data: A general framework. *SIAM Journal on Numerical Analysis*, 33(3):1205–1256, 1996.
- [28] S López-Ureña, JR Torres-Lapasió, R Donat, and MC García-Alvarez-Coque. Gradient design for liquid chromatography using multi-scale optimization. *Journal of Chromatography A*, 1534:32–42, 2018.
- [29] DA Masters, NJ Taylor, TCS Rendall, and Christian B Allen. Multilevel subdivision parameterization scheme for aerodynamic shape optimization. *AIAA Journal*, 55(10):3288–3303, 2017.
- [30] Stephen G Nash. A multigrid approach to discretized optimization problems. *Optimization Methods and Software*, 14(1-2):99–116, 2000.

A On the Property S for subdivision schemes

For completeness, in this section we provide a proof, without entering into too many details, which is well-known in subdivision schemes theory.

Lemma 3. *Let $\mathcal{P} = (P_k^{k+1})_{k=0}^\infty$ be the sequence of linear, interpolatory, prediction operators defined in Section 2.1. Then there exists $C > 0$ such that*

$$\|\varepsilon^\ell\|_\infty \leq \|P_\ell^k \varepsilon^\ell\|_\infty \leq C \|\varepsilon^\ell\|_\infty, \quad \forall 0 \leq \ell \leq k.$$

Proof. Any interpolatory prediction operator fulfills

$$\|\varepsilon^\ell\|_\infty = \sup_{0 \leq i \leq J_\ell} |\varepsilon_i^\ell| = \sup_{0 \leq i \leq J_\ell} |(P_\ell^{\ell+1} \varepsilon^\ell)_{2i}| \leq \sup_{0 \leq i \leq J_{\ell+1}} |(P_\ell^{\ell+1} \varepsilon^\ell)_i| = \|P_\ell^{\ell+1} \varepsilon^\ell\|_\infty.$$

Applying this inductively, we obtain the first inequality

$$\|\varepsilon^\ell\|_\infty \leq \|P_\ell^{\ell+1} \varepsilon^\ell\|_\infty \leq \|P_{k-1}^k \cdots P_\ell^{\ell+1} \varepsilon^\ell\|_\infty = \|P_\ell^k \varepsilon^\ell\|_\infty.$$

The second inequality is a consequence of the fact that the subdivision process associated to the recursive application of the predictions operators is convergent (see e.g. [21, 4, 17]), which means that for each vector ε^ℓ there exists a continuous function, which we denote by $P_\ell^\infty \varepsilon^\ell \in \mathcal{C}([0, 1], \mathbb{R})$, such that

$$\lim_{\ell < m \rightarrow \infty} \sup_{0 \leq i \leq J_m} |(P_\ell^m \varepsilon^\ell)_i - (P_\ell^\infty \varepsilon^\ell)(h_m i)| = 0,$$

with $h_m = J_m^{-1}$ being the grid spacing at m -level. For interpolatory prediction operators $(P_\ell^k \varepsilon^\ell)_i = (P_\ell^\infty \varepsilon^\ell)(h_k i)$, $0 \leq i \leq J_k$, $0 \leq k$, by the interpolation condition, hence

$$\|P_\ell^k \varepsilon^\ell\|_\infty = \sup_{0 \leq i \leq J_k} |(P_\ell^k \varepsilon^\ell)_i| = \sup_{0 \leq i \leq J_k} |(P_\ell^\infty \varepsilon^\ell)(h_k i)| \leq \sup_{t \in [0, 1]} |(P_\ell^\infty \varepsilon^\ell)(t)|.$$

Since $\varepsilon^\ell = \sum_{i=0}^{J_\ell} \varepsilon_i \delta_i^\ell$, with δ_i^ℓ the canonical i -th vector in \mathbb{R}^{N_ℓ} , and the prediction operators are linear, the result will follow from the properties of the limit functions $\phi_i^\ell = P_\ell^\infty \delta_i^\ell$. It can be proven (see [4, 17]) that these limit functions have compact support (narrower than $2nh_\ell$, with n as in Section 2.1) and satisfy a refinability property which ensures that there exists $\tilde{C} > 0$ such that $\|\phi_i^\ell\|_\infty \leq \tilde{C}$, $\forall i, 0 \leq i \leq J_\ell, \forall \ell \geq 0$. Given $\varepsilon^\ell \in \mathbb{R}^{N_\ell}$,

$$P_\ell^\infty \varepsilon^\ell(t) = \sum_{i=0}^{J_\ell} \varepsilon_i^\ell \phi_i^\ell(t), \quad t \in [0, 1] \quad \rightarrow \quad |(P_\ell^\infty \varepsilon^\ell)(t)| \leq \|\varepsilon^\ell\|_\infty \sum_{i=0}^{J_\ell} |\phi_i^\ell(t)|$$

the result follows from observing that for any $t \in [0, 1]$, $\phi_i^\ell(t) \neq 0$ only for at most $2n$ such functions (see [4, 17]). Hence for some $C > 0$, which does not depend on ℓ , the second inequality is obtained. \square

B Limit function basis of the prediction operators

The prediction operators described in section 2.1 are based on n -th degree polynomial interpolation, with $n = 1, 3, 5$. Since they are linear operators, the refined data can be written in terms of a basis. In figs. 8 and 9, some limit function basis for $n = 3, 5$, respectively, are shown.

C Smoothness of the MINS and MOREBV solutions

In this section we discuss about the regularity of the solutions to the problems ‘MINS’ eq. (45) and ‘MOREBV’ eq. (46).

According the boundary conditions, the derivatives $\frac{\partial^3}{\partial x^3}$ $\frac{\partial^3}{\partial y^3}$ of the solution u to the continuous problem must be zero in the four corners $(0, 0), (1, 0), (0, 1), (1, 1)$. In the pictures in fig. 10 there is a sudden change in the value of the derivatives in the corners. On the one direction (x or y , depending on the picture), the derivative is zero, while in the other direction, the absolute value grows when approaching to the corner. If there exists some continuous function which point evaluations are the discrete solution z_{\min} , then its third derivatives seem to be not continuous in the four corners. Hence, the solutions are not C^3 globally. For comparison, we show the graphics of $\frac{\partial^2}{\partial x^2}$ $\frac{\partial^2}{\partial y^2}$ in Figure fig. 11, which seem to be continuous, but not differentiable.

D Sub-optimal solutions of the MOREBV problem

In this section we show the sub-optimal solutions found by MR/OPT when solving the MOREBV problem as in section 4.2.

Observe in fig. 12 that, for the linear prediction operators in section 2.1 with $n = 1$, how slowly the sub-optimal solutions approaches the solution (pay attention to the z -axis). The low regularity of the data generated by this prediction operators may explain this behavior, since the continuous optimization problem requires the computation of a Laplacian.

However, we can see in figs. 13 and 14 that for $n = 3, 5$ the sub-optimal solution converges quickly to z_{\min} .

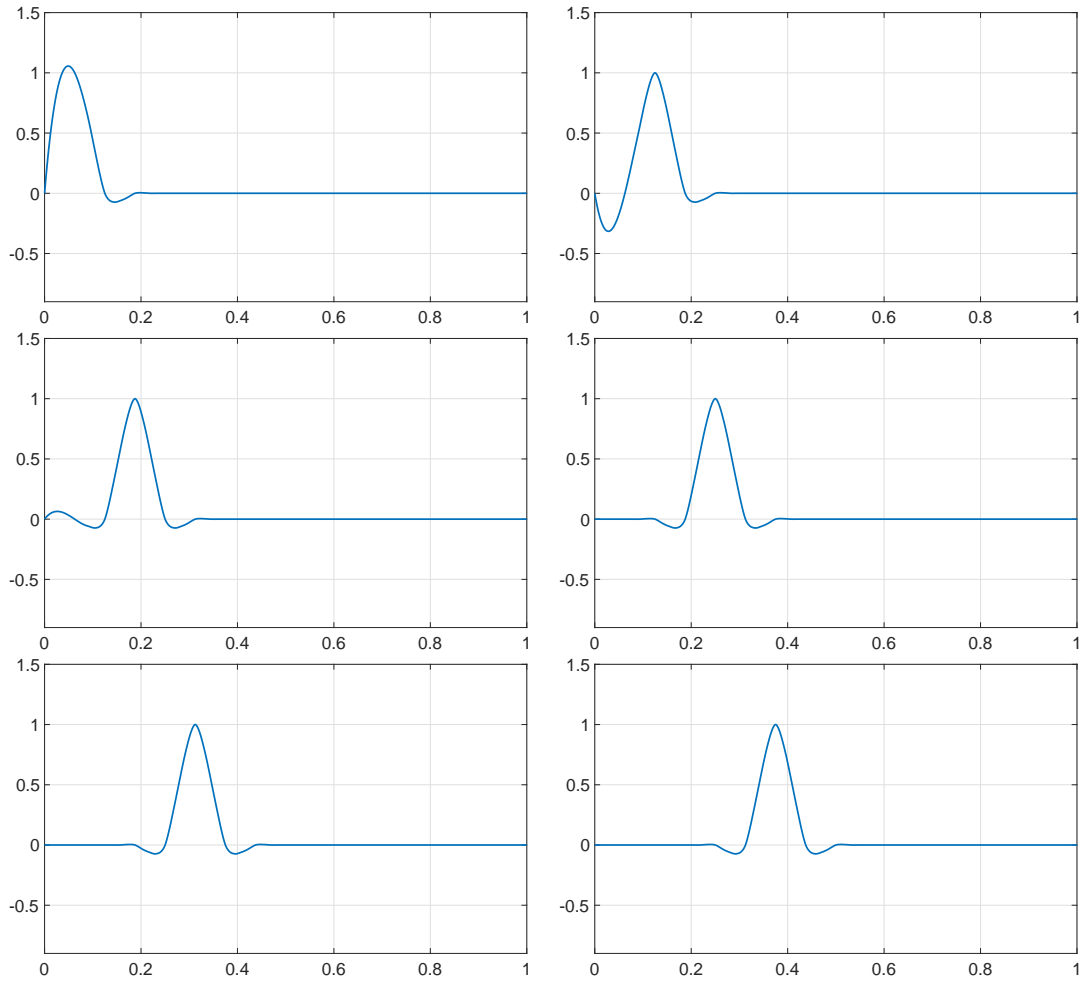


Figure 8: Some of the basis functions for the space of generated functions by the prediction schemes in section 2.1 for $n = 3$. The starting level has 17 equal-spaced nodes in $[0,1]$, and the prediction operators are applied 10 times, so the final level has grid points.

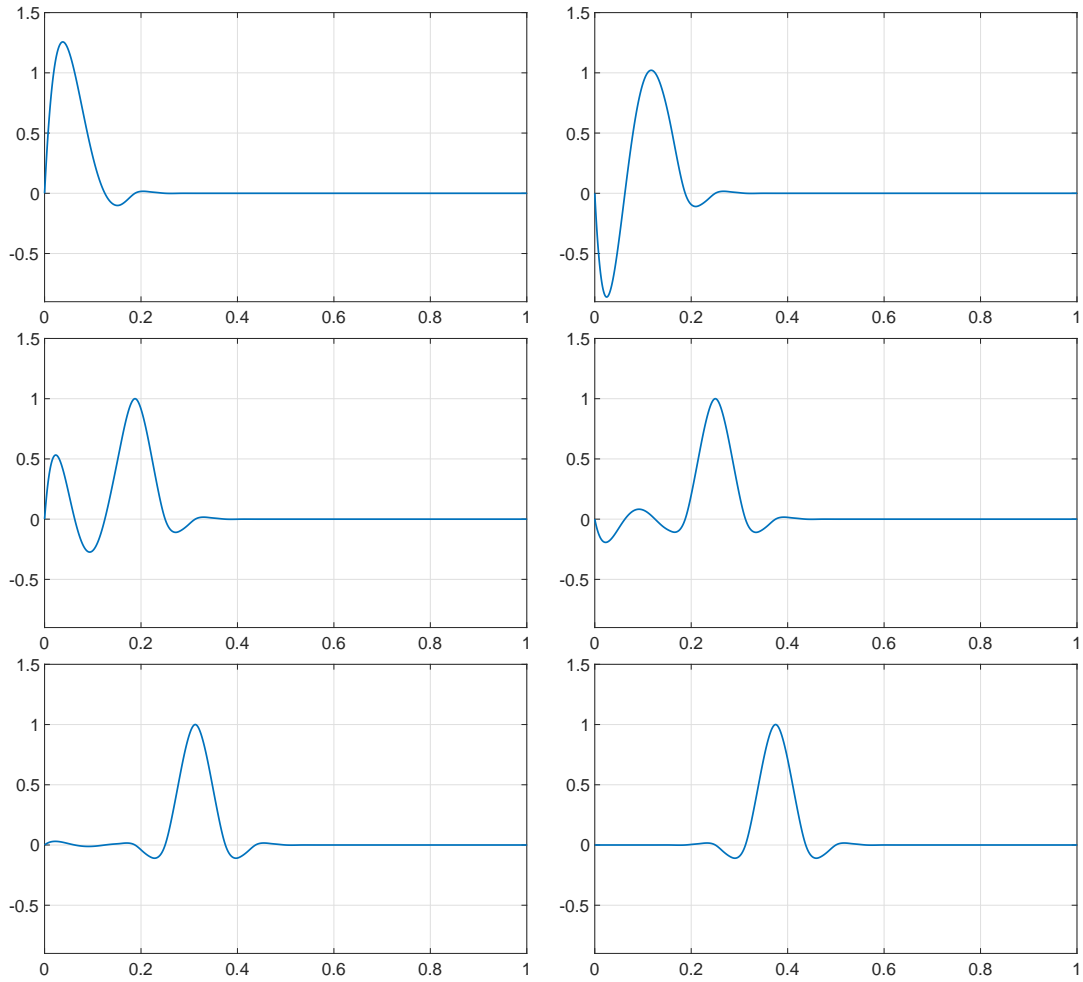


Figure 9: Some of the basis functions for the space of generated functions by the prediction schemes in section 2.1 for $n = 5$. The starting level has 17 equal-spaced nodes in $[0,1]$, and the prediction operators are applied 10 times, so the final level has 65537 grid points.

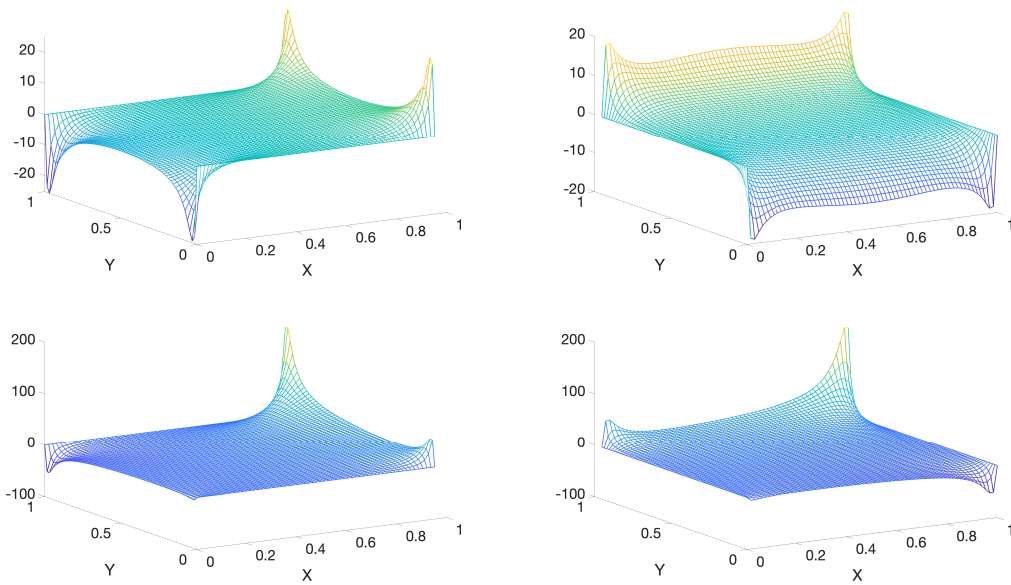


Figure 10: The derivatives $\frac{\partial^3}{\partial x^3}$ $\frac{\partial^3}{\partial y^3}$ (left and right columns, respectively) in the interval $[0, 1] \times [0, 1]$ of the solutions to the problems ‘MINS’ eq. (45) and ‘MOREBV’ eq. (46) (top and bottom rows). The solutions were computed on a 65×65 uniform grid up to machine precision, solving the minimization problem with the direct use of `fminunc`.

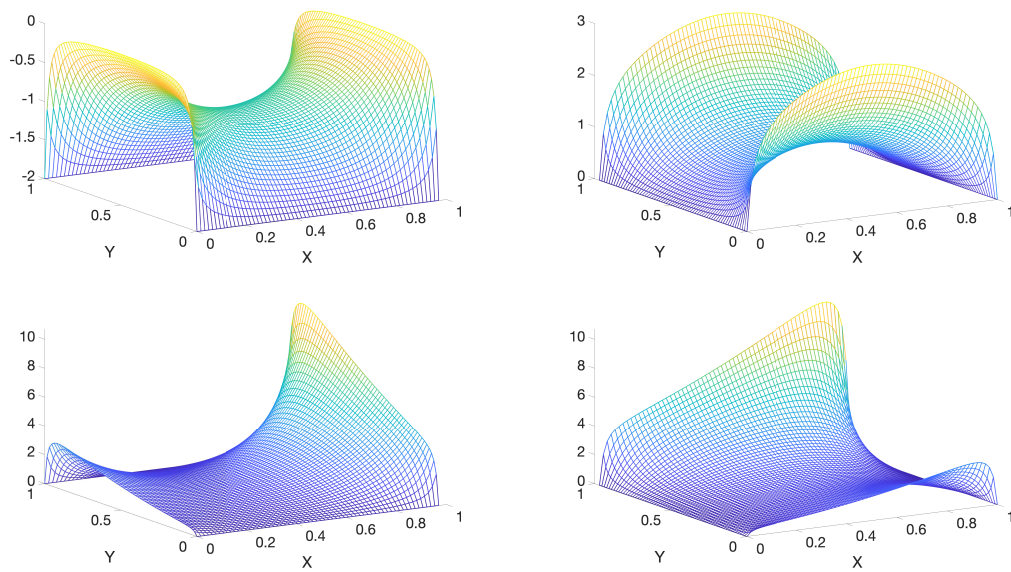


Figure 11: The derivatives $\frac{\partial^2}{\partial x^2}$ $\frac{\partial^2}{\partial y^2}$ (left and right columns, respectively) in the interval $[0, 1] \times [0, 1]$ of the solutions to the problems ‘MINS’ eq. (45) and ‘MOREBV’ eq. (46) (top and bottom rows). The solutions were computed on a 65×65 uniform grid up to machine precision, solving the minimization problem with the direct use of `fminunc`.

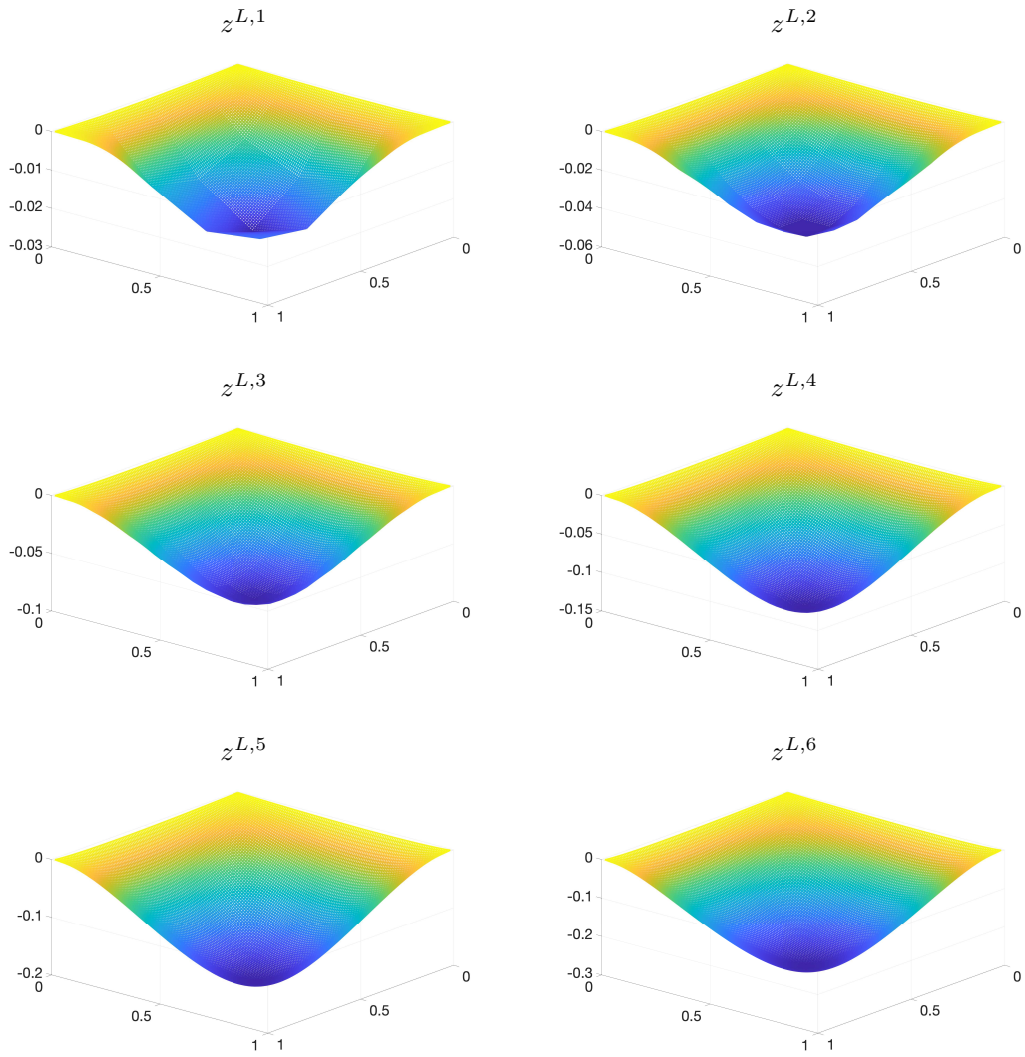


Figure 12: The suboptimal solutions to the problem ‘MOREBV’ eq. (46) for $n = 1$.

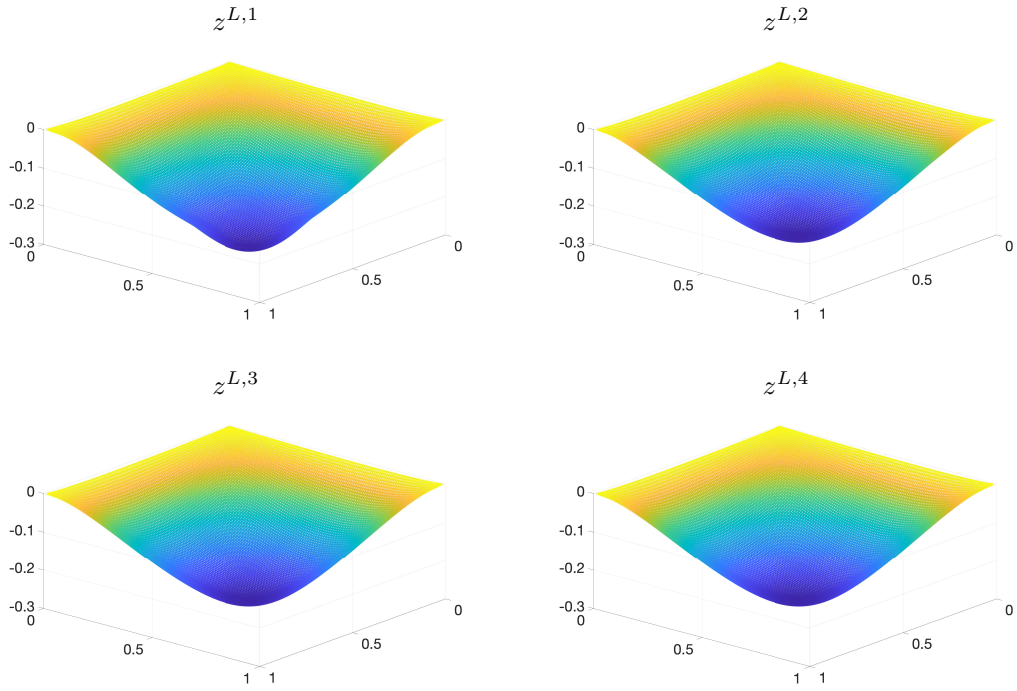


Figure 13: Some suboptimal solutions to the problem 'MOREBV' eq. (46) for $n = 3$.

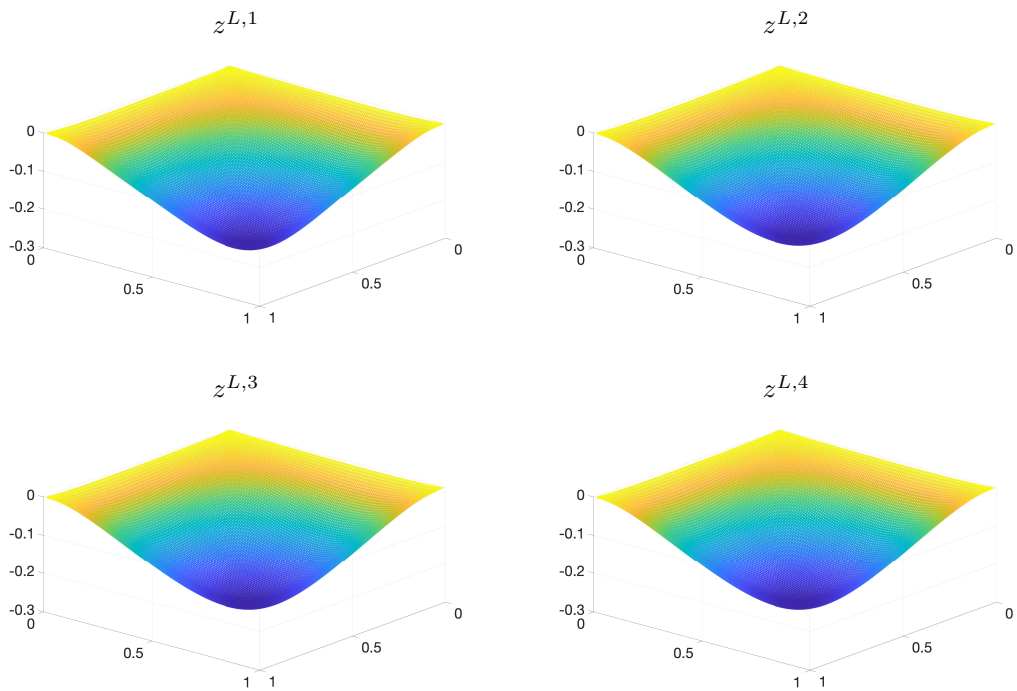


Figure 14: Some suboptimal solutions to the problem 'MOREBV' eq. (46) for $n = 5$.